Magnetic-field- and hyperfine-induced $^3P_0$-$^1S_0$ transitions in Be- and Ne-like ions

Wenxian Li,[1,*] Per Jönsson,[1] Tomas Brage,[2,3,†] and Roger Hutton[3,‡]

[1]*Faculty of Technology and Society, Department of Materials Science and Applied Mathematics, Malmö University, 205-06 Malmö, Sweden*

[2]*Division of Mathematical Physics, Department of Physics, Lund University, 221-00 Lund, Sweden*

[3]*Institute of Modern Physics, Fudan University, Shanghai 200433, People's Republic of China*

(Received 24 July 2017; published 28 November 2017)

In this work, we investigate the magnetic-field- and hyperfine-induced $^3P_0 \rightarrow {}^1S_0$ transitions in Be- and Ne-like ions along the respective isoelectronic sequence by using the multiconfiguration Dirac-Hartree-Fock method. The transition probabilities are in this case dependent on the magnetic hyperfine quantum number M_F of the upper state. We show that it is important to include perturbers with $\Delta F = \pm 1$. The calculated transition rates are compared to experimental results, when available. The discrepancies between the resulting magnetic-field- and hyperfine-induced transition rates and the experimental values in Be-like ions are discussed as well as the observability of the hyperfine-induced transitions in Ne-like ions.

DOI: 10.1103/PhysRevA.96.052508

I. INTRODUCTION

Unexpected transitions [1,2], e.g., spin-, hyperfine- (HIT), and magnetic-field-induced (MIT) transitions, are important in the diagnostics of different plasmas since they are sensitive and unique tools for the determination of, e.g., electron densities, isotope compositions, and magnetic fields [3–5]. These transitions pose a challenge to computations since their predictions often require a careful and thorough treatment of the atomic structure. However, when accurate and systematic methods to calculate their rates are used, theoretical predictions are in agreement with available experimental values for most ions, but some differences still remain.

The MITs have so far been investigated mainly for isotopes without nuclear spin, when the HIT is absent, but in the presence of an external magnetic field, where the interaction with the field breaks the symmetry of the atomic system and opens up magnetic-field-induced transitions. To distinguish these cases from when hyperfine interaction is present, we label them MIT-fs. The theory for these has been discussed in recent publications for Be-, Ne-, and Cl-like ions [6–8].

An MIT was first observed in Ne-like Ar, as the $2p^5 3s\ ^3P_0 \rightarrow 2p^6\ ^1S_0$ transition, by Beiersdorfer *et al.* [9], who also discussed the use of this transition as a diagnostic tool for magnetic fields in plasmas. More recently, the same transition was observed for the Ne-like Fe by the same group [10]. The experimental results for the MIT-fs rates of Ne-like ions are in good agreement with previous theoretical predictions [6]. Recently, it was also proposed that MIT-fs in Cl-like Fe could be used to probe the solar coronal magnetic field [8,11].

Hyperfine-induced transitions (HITs) have low rates and are only present for isotopes with nuclear spin and can therefore be important for diagnostics of isotopic compositions for extremely low density plasmas [3]. A number of recent papers present rates of HITs [3,12–20] in the absence of magnetic fields. For HIT, experimental and theoretical studies for He-like ions [21–29] and Ni-like Xe [15,30–32] are in good agreement. The resulting rate for Be-like N by Brage *et al.* [33], obtained by modeling of a planetary nebulae, are also in agreement with theory, albeit with fairly large experimental uncertainty.

The measured rate for Be-like S by Schippers *et al.* [34] also appears to agree with theoretical work within the experimental uncertainties. At the same time, there are significant discrepancies for Be-like Ti by Schippers *et al.* [35] and Mg-like Al by Rosenband *et al.* [36] between the computed and the experimental HIT rates and the reason for these discrepancies remains unclear. It is clear that in these measurements, performed at storage rings, there are magnetic fields present, the effect of which has to be included in the calculations. The simultaneous inclusion of MIT and HIT, in what we will label MIT-hfs transitions, is the object of this paper.

II. COMPETITION BETWEEN HIT AND MIT

When atoms with nuclear spin are in a magnetic field, the magnetic and hyperfine interactions will contribute to the atomic system simultaneously. To compare the size of different interactions, and predict when these can become important, we present theoretical rates for the different transition channels from the $^3P_0$ to lower states (see the schematic energy-level diagram and denotation of transition channels in Fig. 1) for Be-like ($7 \leqslant Z \leqslant 73$) and Ne-like ($11 \leqslant Z \leqslant 35$) ions in Fig. 2, where the MIT-fs rates are plotted for a range of field strengths. As can be seen from this figure, for Be-likes ions, HIT rates dominate over the MIT-fs channel for ions with larger nuclear charge, even at the strong magnetic field of 12 T. For the ions at the neutral end of the isoelectronic sequence, the rates of the two transition channels are, in general, of comparable size in the given magnetic-field strength region. However, we do have to remember that the HIT rate is given for the most abundant isotope with nuclear spin. In the case of even nuclei, this is usually not the most abundant isotope overall. As an example, consider Be-like C or O, where the nonspin isotopes completely dominate. In these cases, MIT

*Present address: High Altitude Observatory, National Center for Atmospheric Research, P. O. Box 3000, Boulder CO 80307-3000, USA.

†tomas.brage@fysik.lu.se

‡rhutton@fudan.edu.cn

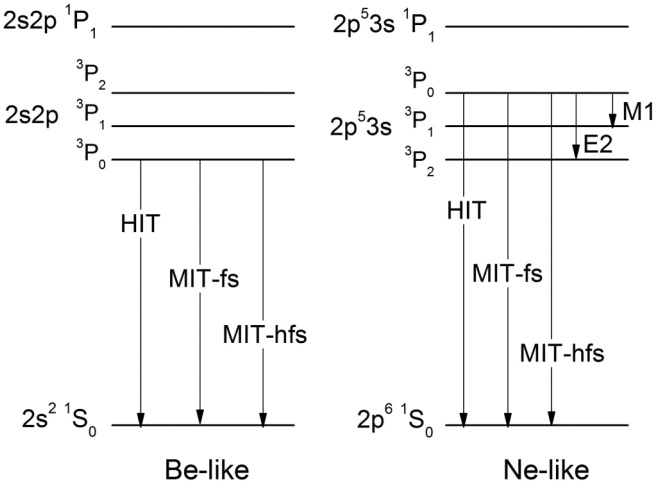

FIG. 1. Schematic energy-level diagram of Be- and Ne-like ions in the LS-coupled, low-Z region of the two isoelectronic sequences, showing possible one-photon transition channels from the $^3P_0$: MIT-fs implies magnetic-field-induced transition for isotopes without nuclear spin ($I = 0$), HIT refers to hyperfine-induced transition without external magnetic field, and MIT-hfs: magnetic-field- and hyperfine-induced transitions for isotopes with nuclear spin ($I \neq 0$). M1 and E2 are forbidden magnetic dipole and electric quadrupole transitions, respectively.

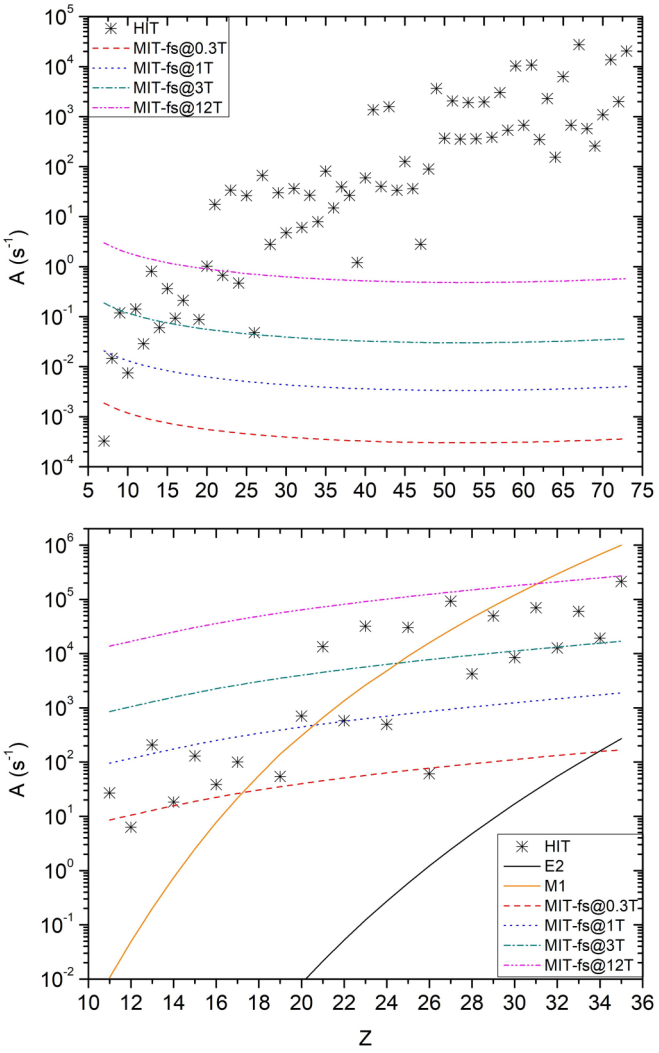

FIG. 2. Rates of transitions from the $^3P_0$ (notation is defined in Fig. 1) in Be-like ($7 \leqslant Z \leqslant 73$, upper panel) and Ne-like ($11 \leqslant Z \leqslant 35$, lower panel) ions. The MIT-fs are given in the magnetic field of 0.3, 1, 3, and 12 T. The E2 transitions are ignored for the ions with the rates smaller than 10^{-2} s^{-1}. The y axis is given in logarithmic scale. Note: The HIT rates are from the most abundant isotopes with nuclear spin.

are the most important decay channel for the most abundant isotope.

The plot for Ne-like ions shows the competitive decay channels along the isoelectronic sequence. At the low-Z end of the sequence, the HIT and MIT-fs are of, again, comparable size, even in the relatively weak magnetic-field region, while for the higher-Z ions they reach comparable size at higher magnetic-field strengths due to the Z dependence of HIT rates and the B^2 dependence of MIT-fs rates. The M1 transition rate has a stronger Z dependence, and it is comparable in size with the HIT rate for the high-Z end. The electric quadrupole (E2) transition $^3P_0$-$^3P_2$ has a rate that is between three and four orders of magnitude smaller than M1 transition to $^3P_0$ level. Figure 2 clearly shows that the contribution from the magnetic field must be taken into account carefully to properly extract the HIT rate from measurements in the existence of a magnetic field for a large range of magnetic fields. At the same time, it is clear that HIT is the dominant decay channel in the absence of an external magnetic field for a large range of odd nuclear charge.

Since there are magnetic fields associated with storage rings, Li *et al.* [37] investigated the contribution of the magnetic fields to the HIT rate for Be-like Ti and concluded that these effects were too weak at the experimental magnetic flux density of 0.75 T. However, in their calculation they neglected the mixing from the $\Delta F \neq 0$ perturbers, which could be important for higher field strengths. A first more systematic and complete investigation of what we will label MIT-hfs, the simultaneous inclusion of HIT and MIT to compute transition rates, for isotopes with nuclear spin, is the aim of this work.

III. THEORETICAL METHOD

A. General theory

1. Hyperfine interaction

The Hamiltonian of an atom with a nuclear spin I ($\neq 0$) can be written as

$$H = H_{fs} + H_{hfs}, \tag{1}$$

where H_{fs} is the relativistic fine-structure Hamiltonian including the Breit interaction in the low-frequency limit and estimates of the quantum electrodynamical (QED) effects, while H_{hfs} is the interaction between the electrons and the nonspherical electromagnetic multipole moments of the nucleus. The latter interaction can be written as a multipole

expansion

$$H_{hfs} = \sum_{k=1} \mathbf{T}^{(k)} \cdot \mathbf{M}^{(k)}, \tag{2}$$

where $\mathbf{T}^{(k)}$ and $\mathbf{M}^{(k)}$ are spherical tensor operators of rank k in the electronic and nuclear spaces, respectively. The hyperfine interaction couples the total electronic angular momentum $\mathbf{J}$ and the nuclear momentum $\mathbf{I}$ to a new total angular momentum $\mathbf{F}$. In this model, only F and M_F are good quantum numbers, and the wave function can be expressed as an expansion

$$|\Upsilon\tilde{\Gamma} F M_F\rangle = \sum_{\Gamma J} d_{\Gamma J} |\Upsilon \Gamma I J F M_F\rangle, \tag{3}$$

where $|\Upsilon\Gamma I J F M_F\rangle$ are IJF-coupled products of unperturbed nuclear $|\Upsilon I M_I\rangle$ and electronic $|\Gamma J M_J\rangle$ wave functions. The expansion coefficients $d_{\Gamma J}$ are obtained by setting up and diagonalizing the interaction matrix. The matrix elements of H_{fs} are diagonal, defining the "unperturbed" fine-structure energies. The matrix elements for the leading terms of the hyperfine interaction H_{hfs} can be expressed as a product of reduced electronic and nuclear matrix elements. The first is the magnetic dipole term

$$\begin{aligned}&\langle \Upsilon\Gamma I J F M_F | \mathbf{T}^{(1)} \cdot \mathbf{M}^{(1)} | \Upsilon\Gamma' I J' F M_F\rangle \\ &= (-1)^{I+J+F} \begin{Bmatrix} I & J & F \\ J' & I & 1 \end{Bmatrix} \sqrt{2J+1}\sqrt{2I+1} \\ &\quad \times \langle \Gamma J || \mathbf{T}^{(1)} || \Gamma' J' \rangle \langle \Upsilon I || \mathbf{M}^{(1)} || \Upsilon I \rangle,\end{aligned} \tag{4}$$

where $J' = J-1, J$, and the second is the electric quadrupole term

$$\begin{aligned}&\langle \Upsilon\Gamma I J F M_F | \mathbf{T}^{(2)} \cdot \mathbf{M}^{(2)} | \Upsilon\Gamma' I J' F M_F\rangle \\ &= (-1)^{I+J+F} \begin{Bmatrix} I & J & F \\ J' & I & 2 \end{Bmatrix} \sqrt{2J+1}\sqrt{2I+1} \\ &\quad \times \langle \Gamma J || \mathbf{T}^{(2)} || \Gamma' J' \rangle \langle \Upsilon I || \mathbf{M}^{(2)} || \Upsilon I \rangle,\end{aligned} \tag{5}$$

where $J' = J-2, J-1, J$. The nuclear matrix elements in these expressions can be related to the parameters μ_I and Q according to

$$\langle \Upsilon I || \mathbf{M}^{(1)} || \Upsilon I \rangle = \mu_I \sqrt{\frac{I+1}{I}} \tag{6}$$

and

$$\langle \Upsilon I || \mathbf{M}^{(2)} || \Upsilon I \rangle = \frac{1}{2} Q \sqrt{\frac{(2I+1)(I+1)}{I(2I-1)}}. \tag{7}$$

Since the hyperfine interaction operator H_{hfs} does not commute with $\mathbf{J}$, the off-diagonal hyperfine interaction introduces mixing between unperturbed electronic levels with different J quantum numbers opening up new transition channels, labeled hyperfine-induced transitions (HIT).

More details about the hyperfine interaction and the matrix elements can be found in Refs. [3,14–16,38,39].

2. Magnetic interaction on fine-structure levels

If we choose the direction of the magnetic field as the z direction, the Hamiltonian of atoms with zero nuclear spin in the presence of an external magnetic field can be written as

$$H = H_{fs} + H_m = H_{fs} + \left(N_0^{(1)} + \Delta N_0^{(1)}\right) B, \tag{8}$$

where H_m is the interaction Hamiltonian with the external magnetic field. The tensor operator $\mathbf{N}^{(1)}$ represents the coupling of the electrons with the field, and $\Delta\mathbf{N}^{(1)}$ is the Schwinger QED correction [40]. Now, only M_J remains a good quantum number, and the wave function is written as an expansion

$$|\tilde{\Gamma} M_J\rangle = \sum_{\Gamma J} d_{\Gamma J} |\Gamma J M_J\rangle. \tag{9}$$

Again, the expansion coefficients $d_{\Gamma J}$ are obtained by setting up and diagonalizing the interaction matrix. The magnetic interaction matrix elements can be expressed in terms of the reduced electronic matrix elements and the magnetic field

$$\begin{aligned}&\langle \Gamma J M_J | N_0^{(1)} + \Delta N_0^{(1)} | \Gamma' J' M_J\rangle \\ &= (-1)^{J-M_J} \begin{pmatrix} J & 1 & J' \\ -M_J & 0 & M_J \end{pmatrix} \sqrt{2J+1} \\ &\quad \times \langle \Gamma J || \mathbf{N}^{(1)} + \Delta\mathbf{N}^{(1)} || \Gamma' J' \rangle,\end{aligned} \tag{10}$$

where $J' = J-1, J$. Just as for the hyperfine structure there is a mixing between unperturbed electronic levels with different J quantum numbers.

More details about magnetic interaction and the evaluation of the matrix elements can be found in Ref. [41].

3. Magnetic interaction of hyperfine levels

In the presence of an external magnetic field B, the Hamiltonian of an atom with nuclear spin I ($\neq 0$) can be expressed as

$$H = H_{fs} + H_{hfs} + H_m. \tag{11}$$

In this case, M_F is the only good quantum number and the wave function can be expressed as the expansion

$$|\Upsilon\tilde{\Gamma} I M_F\rangle = \sum_{\Gamma J F} d_{\Gamma J F} |\Upsilon\Gamma I J F M_F\rangle. \tag{12}$$

The expansion coefficients are obtained again by setting up and diagonalizing the interaction matrix. The hyperfine interaction matrix elements in Eqs. (4) and (5) are diagonal in $\mathbf{F}$. The magnetic interaction Hamiltonian can now be written as

$$H_m = \left(N_0^{(1)} + \Delta N_0^{(1)}\right) B + H_m^{\text{nuc}}, \tag{13}$$

where the last term, H_m^{nuc}, represents the interaction of the magnetic field with the magnetic moment of the nucleus. This is weak and can be neglected for the systems discussed here. The magnetic interaction matrix elements between the coupled atomic and nuclear wave functions are, for (i) diagonal elements in F,

$$\begin{aligned}&\langle \Upsilon\Gamma I J F M_F | N_0^{(1)} + \Delta N_0^{(1)} | \Upsilon\Gamma' I J' F M_F\rangle \\ &= (-1)^{I+J'+1+F} M_F \sqrt{\frac{2F+1}{F(F+1)}} \begin{Bmatrix} J & F & I \\ F & J' & 1 \end{Bmatrix} \\ &\quad \times \sqrt{2J+1} \langle \Gamma J || \mathbf{N}^{(1)} + \Delta\mathbf{N}^{(1)} || \Gamma' J' \rangle,\end{aligned} \tag{14}$$

where $J' = J-1, J$, and for (ii) nondiagonal elements,

$$\langle \Upsilon\Gamma I J F M_F | N_0^{(1)} + \Delta N_0^{(1)} | \Upsilon\Gamma' I J' F - 1 M_F \rangle = (-1)^{I+J'+1+F} \sqrt{\frac{F^2 - M_F^2}{F}} \begin{Bmatrix} J & F & I \\ F-1 & J' & 1 \end{Bmatrix} \times \sqrt{2J+1} \langle \Gamma J || \mathbf{N}^{(1)} + \Delta \mathbf{N}^{(1)} || \Gamma' J' \rangle, \quad (15)$$

where $J' = J-1, J, J+1$. Two things should be noted. First, as shown in Eqs. (14) and (15), the magnetic interaction matrix element between states with the same F values depends on M_F instead of $|M_F|$, while that with $\Delta F = 1$ depends on absolute value of M_F. It means that when the two mixing cases above occur simultaneously, they yield different mixing coefficients for M_F and $-M_F$ states, which we will see leads to different transition rates. Second, when the hyperfine and magnetic interactions contribute simultaneously, the expansion coefficients in Eq. (12) are no longer linear in B due to the inclusion of H_{hfs} into the Hamiltonian. As an example, when there is destructive interference between the contributions from the hyperfine and magnetic interactions, there may be a nonmonotonic change of, e.g., rates as a function of the magnetic-field strength.

4. Induced transitions

There are a wide range of calculations for hyperfine-induced transitions (HIT) [3,12,14–16,19,20,39,42] and magnetic-field-induced transitions for isotopes without nuclear spin (MIT-fs) [2,6,8]. Here, we focus on discussing the magnetic-field- and hyperfine-induced (MIT-hfs) transitions for isotopes with nuclear spin. The transition probability for an electric dipole transition between two magnetic subhyperfine levels is given by

$$A(\widetilde{\Gamma} M_F, \widetilde{\Gamma}' M_F') = \frac{2.02613 \times 10^{18}}{\lambda^3} \sum_q |\langle \widetilde{\Gamma} M_F | P_q^{(1)} | \widetilde{\Gamma}' M_F' \rangle|^2, \quad (16)$$

where A is in s^{-1} and λ is the wavelength of the transition in Å. Substituting Eq. (12) into Eq. (16) and using the Wigner-Eckart theorem, we get

$$\begin{aligned} A(\widetilde{\Gamma} M_F, \widetilde{\Gamma}' M_F') &= \frac{2.02613 \times 10^{18}}{\lambda^3} \sum_q \left| \sum_{\Gamma J F} \sum_{\Gamma' J' F'} d_{\Gamma J F} d_{\Gamma' J' F'} \right. \\ &\quad \left. \times \langle \Gamma J F M_F | P_q^{(1)} | \Gamma' J' F' M_F' \rangle \right|^2 \\ &= \frac{2.02613 \times 10^{18}}{\lambda^3} \sum_q \left| \sum_{\Gamma J F} \sum_{\Gamma' J' F'} d_{\Gamma J F} d_{\Gamma' J' F'} \sqrt{2F'+1} \right. \\ &\quad \times \sqrt{2F+1} \begin{pmatrix} F & 1 & F' \\ -M_F & q & M_F' \end{pmatrix} \begin{Bmatrix} J & F & I \\ F' & J' & 1 \end{Bmatrix} \\ &\quad \left. \times \langle \Gamma J || \mathbf{P}^{(1)} || \Gamma' J' \rangle \right|^2. \end{aligned} \quad (17)$$

As an example, for the Be-like system, under the influence of an external magnetic field for isotopes with nuclear spin, the reference state $|\text{“}2s2p\,^3P_0\text{”}\rangle$ can be expressed as

$$|\text{“}2s2p\,^3P_0\text{”} I M_F' \rangle = d_0 |2s2p\,^3P_0 I F(=I) M_F' \rangle + \sum_{S=1,3;F'} d_{S,F'} |2s2p\,^S P_1 I F' M_F' \rangle, \quad (18)$$

where $F' = F-1$, F, and $F+1$. The interactions with $|\text{“}2s2p\,^3P_2\text{”} I M_F' \rangle$ and with other atomic states can be neglected since their interaction with the $J=0$ state is weak. The ground state $|\text{“}2s^2\,^1S_0\text{”}\rangle$, which is isolated in energy, can be written as

$$|\text{“}2s^2\,^1S_0\text{”} I M_F \rangle = |2s^2\,^1S_0\, I F(=I) M_F \rangle. \quad (19)$$

Substituting Eqs. (18) and (19) into Eq. (17) and applying standard tensor algebra, we obtain the total transition rate from $|\text{“}2s2p\,^3P_0\text{”} M_F' \rangle$ to the ground state $|\text{“}2s^2\,^1S_0\text{”}\rangle$ as

$$A(M_F') = \sum_{M_F} A(M_F' - M_F) = \frac{2.02613 \times 10^{18}}{3\lambda^3} \left| \sum_{S=1,3} d_S \langle 2s^2\,^1S_0 || \mathbf{P}^{(1)} || 2s2p\,^S P_1 \rangle \right|^2, \quad (20)$$

where the dependence on μ_I, Q, I, F', M_F', and B has been absorbed in the mixing coefficients d_S. The expression of the MIT-hfs transition rate above has the same appearance as the one for HIT and MIT-fs. The difference is in the mixing coefficients d_S due to the incorporation of different interactions into the Hamiltonian.

B. MCDHF method

The electronic wave functions are computed using the latest GRASP2K program package [43] which is based on the multiconfiguration Dirac-Hartree-Fock (MCDHF) method [44,45]. Here, the atomic state functions (ASFs) were obtained as linear combinations of configuration state functions (CSFs)

$$|\Gamma J M_J \rangle = \sum_i c_i |\gamma_i J M_J \rangle, \quad (21)$$

where J and M_J are the angular and magnetic quantum numbers, c_i stands for the mixing coefficients, and γ_i denotes all the other coupling information needed to uniquely define the state. Both the radial parts of the Dirac orbitals and the expansion coefficients c_i are optimized in a self-consistent field procedure using the Dirac-Coulomb Hamiltonian. The Breit interaction and leading quantum electrodynamic (QED) corrections effects, in the form of self-energy and vacuum polarization, are included in a subsequent relativistic configuration interaction (RCI) calculation [43,46].

To derive induced transition rates, we need to calculate the transition probabilities in Eq. (20) as well as the hyperfine and magnetic interaction matrix elements [2]. The transition rates can be expressed in both the Babushkin and Coulomb gauges [47]. In the case of exact wave functions, the two gauges should give the same results. But, it is common that especially

for weak transitions, the matrix elements differ substantially due to neglected contributions from the negative energy part of the electronic wave function to the matrix element in the Coulomb gauge [48]. For this reason, transition rates are all given in Babushkin gauge in this work. The reduced hyperfine and magnetic interaction matrix elements, needed for the determining the mixing coefficients d_S, are calculated using the GRASP2K module HFSZEEMAN [41].

C. Correlation model

The calculations for Be- and Ne-like ions are both based on the restricted active space method [49–51]. The method is applied in a layer-by-layer scheme in which the active set of one-electron Dirac orbitals is expanded systematically until the results show convergence. This allows for a systematic approach to predict rates for the induced transitions.

1. Be-like ions

In the calculations for Be-like ions, we use the same strategy as described in Refs. [7,52]. The even-parity, $1s^2 2s^2\ ^1S_0$, and the odd-parity, $1s^2 2s 2p\ ^3P_{0,1,2}, ^1P_1$, states are optimized in two separate calculations. For the MCDHF calculations, the CSF expansions are generated by single, double, triple, and quadruple (SDTQ) excitations to an active set of orbitals with $n \leqslant 4$ ($l \leqslant f$), followed by single (S) and double (D) excitations to orbital sets with higher n, from the multireference (MR) $1s^2 2s^2, 1s^2 2p^2$ for the even-parity states and the $1s^2 2s 2p$ for the odd states. For the RCI calculation, the CSF expansions are extended, using the same active sets of orbitals as above, but including CSFs generated by triple (T) and quadruple (Q) excitations from the MR to the whole active set, but with the restriction that there should be at least two electrons in subshells with $n \leqslant 3$. The active space for ions with charge states $Z = 5$–42 is expanded up to $n = 8$ ($l = i$), while for $Z = 43$–73 it is sufficient to go to $n = 7$ ($l = i$) to reach convergence of the computed properties. More details and results for other atomic properties can be found in Ref. [52].

2. Ne-like ions

For Ne-like ions we use the computational strategy described in Refs. [6,53]. Single reference configuration models are used both for the even-parity $1s^2 2s^2 2p^6\ ^1S_0$ and the odd-parity $1s^2 2s^2 2p^5 3s\ ^3P_{0,1,2}, ^1P_1$ states. For the MCDHF calculations, the $1s$ shell is kept inactive and the CSF expansions are obtained by SD excitations from the remaining shells to an active set with $n \leqslant 7$ ($l \leqslant i$). At the last step when optimizing $n = 7$ orbitals, we restrict our active space, by only allowing at the most one excitation from $2s$ or $2p$. For the even-parity states, no additional restrictions for the $n = 7$ expansion were imposed. The expansions for the RCI calculations are obtained by extending the CSF expansion by also allowing T excitations from the reference configurations to the active set with $n \leqslant 4$ ($l \leqslant f$) and then SD excitation for $n = 5$–7, again with the $1s$ shell inactive. To allow for the spin polarization of the $1s$ shell, which is essential for the correct treatment of the hyperfine interaction [54], we add at the end all SD excitations, where one of the excitations was from $1s$ and the other from $2s$, $2p$, or $3s$ to $n = 7$. More details can be found in Ref. [53].

TABLE I. Reduced magnetic-field-induced $2s2p\ ^3P_0 \rightarrow 2s^2\ ^1S_0$ transition rates $A^R_{\text{MIT-fs}}$ for Be-like ions ($5 \leqslant Z \leqslant 73$) without nuclear spin. All transition rates are given in $\text{s}^{-1}\,\text{T}^{-2}$ and $a[b]$ represent $a \times 10^b$.

Ions	$A^R_{\text{MIT-fs}}$	Ions	$A^R_{\text{MIT-fs}}$	Ions	$A^R_{\text{MIT-fs}}$
B	3.965[−2]	Ni	4.602[−3]	Sb	3.356[−3]
C	2.696[−2]	Cu	4.474[−3]	Te	3.353[−3]
N	2.081[−2]	Zn	4.357[−3]	I	3.355[−3]
O	1.745[−2]	Ga	4.249[−3]	Xe	3.358[−3]
F	1.500[−2]	Ge	4.151[−3]	Cs	3.366[−3]
Ne	1.317[−2]	As	4.060[−3]	Ba	3.375[−3]
Na	1.177[−2]	Se	3.977[−3]	La	3.389[−3]
Mg	1.065[−2]	Br	3.902[−3]	Ce	3.405[−3]
Al	9.738[−3]	Kr	3.832[−3]	Pr	3.425[−3]
Si	8.980[−3]	Rb	3.769[−3]	Nd	3.448[−3]
P	8.340[−3]	Sr	3.712[−3]	Pm	3.473[−3]
S	7.793[−3]	Y	3.660[−3]	Sm	3.500[−3]
Cl	7.321[−3]	Zr	3.614[−3]	Eu	3.532[−3]
Ar	6.909[−3]	Nb	3.572[−3]	Gd	3.564[−3]
K	6.547[−3]	Mo	3.533[−3]	Tb	3.602[−3]
Ca	6.227[−3]	Tc	3.495[−3]	Dy	3.643[−3]
Sc	5.943[−3]	Ru	3.466[−3]	Ho	3.687[−3]
Ti	5.689[−3]	Rh	3.441[−3]	Er	3.734[−3]
V	5.460[−3]	Pd	3.419[−3]	Tm	3.785[−3]
Cr	5.253[−3]	Ag	3.401[−3]	Yb	3.837[−3]
Mn	5.067[−3]	Cd	3.385[−3]	Lu	3.894[−3]
Fe	4.893[−3]	In	3.367[−3]	Hf	3.951[−3]
Co	4.743[−3]	Sn	3.361[−3]	Ta	4.010[−3]

IV. RESULTS AND DISCUSSIONS

A. MIT-fs

For MIT-fs, the mixing coefficient d_S is proportional to the magnetic-field strength B and the transition rate is therefore proportional to B^2. We define a reduced transition rate $A^R_{\text{MIT-fs}}$, independent of B through

$$A_{\text{MIT-fs}} = A^R_{\text{MIT-fs}} B^2. \tag{22}$$

The reduced transition rate $A^R_{\text{MIT-fs}}$ for Be-like and Ne-like ions are shown in Tables I and II.

TABLE II. Reduced magnetic-field-induced $2p^5 3s\ ^3P_0 \rightarrow 2p^6\ ^1S_0$ transition rates $A^R_{\text{MIT-fs}}$ for Ne-like ions ($11 \leqslant Z \leqslant 35$) without nuclear spin. All transition rates are given in $\text{s}^{-1}\,\text{T}^{-2}$ and $a[b]$ represent $a \times 10^b$.

Ions	$A^R_{\text{MIT-fs}}$	Ions	$A^R_{\text{MIT-fs}}$	Ions	$A^R_{\text{MIT-fs}}$
Na	9.538[1]	Ca	4.445[2]	Cu	1.134[3]
Mg	1.164[2]	Sc	5.028[2]	Zn	1.238[3]
Al	1.426[2]	Ti	5.648[2]	Ga	1.349[3]
Si	1.741[2]	V	6.314[2]	Ge	1.468[3]
P	2.097[2]	Cr	7.024[2]	As	1.595[3]
S	2.492[2]	Mn	7.780[2]	Se	1.732[3]
Cl	2.924[2]	Fe	8.587[2]	Br	1.880[3]
Ar	3.394[2]	Co	9.445[2]		
K	3.901[2]	Ni	1.036[3]		

TABLE III. Hyperfine-induced $2s2p\,^3P_0 \rightarrow 2s^2\,^1S_0$ transition rates $A_{\rm HIT}$ in the absence of an external magnetic field for Be-like ions ($5 \leqslant Z \leqslant 73$) from present calculations and other theoretical works. Nuclear magnetic moments μ_I are from [56]. All transition rates are given in s^{-1} and $a[b]$ represent $a \times 10^b$.

Ions	I	μ_I	Q	$A_{\rm HIT}$	CI [39]	MCDHF [16]	Ions	I	μ_I	Q	$A_{\rm HIT}$	CI [39]
^{11}B	3/2	2.688649	0.04059	2.368[−3]			^{99}Tc	9/2	5.6847	−0.129	1.580[3]	1.574[3]
^{13}C	1/2	0.702412	0	8.319[−4]	8.223[−4]	8.305[−4]	^{99}Ru	5/2	−0.641	0.079	2.675[1]	2.667[1]
^{15}N	1/2	−0.283189	0	3.271[−4]	3.269[−4]	3.285[−4]	^{101}Ru	5/2	−0.719	0.46	3.366[1]	3.350[1]
^{17}O	5/2	−1.89379	−0.0256	1.476[−2]	1.488[−2]	1.478[−2]	^{103}Rh	1/2	−0.884	0	1.266[2]	1.262[0]
^{19}F	1/2	2.628868	0.0942	1.190[−1]	1.208[−1]	1.187[−1]	^{105}Pd	5/2	−0.642	0.66	3.622[1]	3.606[1]
^{21}Ne	3/2	−0.661797	0.102	7.507[−3]	7.453[−3]	7.527[−3]	^{107}Ag	1/2	−0.11357	0	2.817[0]	2.809[0]
^{23}Na	3/2	2.217522	0.104	1.430[−1]	1.431[−1]	1.433[−1]	^{109}Ag	1/2	0.13056	0	3.725[0]	3.712[0]
^{25}Mg	5/2	−0.85545	0.199	2.880[−2]	2.871[−2]	2.893[−2]	^{111}Cd	1/2	−0.594886	0	8.933[1]	8.893[1]
^{27}Al	5/2	3.641507	0.1466	8.095[−1]	8.094[−1]	8.136[−1]	^{113}In	9/2	5.5289	0.759	3.641[3]	3.630[3]
^{29}Si	1/2	−0.55529	0	6.038[−2]	6.011[−2]	6.085[−2]	^{115}Sn	1/2	−0.91883	0	2.842[2]	2.832[2]
^{31}P	1/2	1.1316	0	3.657[−1]	3.648[−1]	3.687[−1]	^{117}Sn	1/2	−1.00104	0	3.372[2]	3.361[2]
^{33}S	3/2	0.643821	−0.0678	9.342[−2]	9.315[−2]	9.439[−2]	^{119}Sn	1/2	−1.04728	0	3.691[2]	3.678[2]
^{35}Cl	3/2	0.821874	−0.817	2.119[−1]	2.113[−1]	2.145[−1]	^{121}Sb	5/2	3.3634	−0.543	2.061[3]	2.045[3]
^{37}Cl	3/2	0.684124	−0.0644	1.468[−1]	1.464[−1]	1.486[−1]	^{123}Sb	7/2	2.5498	−0.692	1.089[3]	1.083[3]
^{39}K	3/2	0.39147	0.0585	8.822[−2]	8.873[−2]	8.974[−2]	^{125}Te	1/2	−0.888505	0	3.536[2]	3.523[2]
^{41}K	3/2	0.21487	0.0711	2.658[−2]	2.673[−2]	2.704[−2]	^{127}I	5/2	2.81327	−0.696	1.917[3]	1.909[3]
^{43}Ca	7/2	−1.3173	−0.0408	1.020[0]	1.021[0]	1.040[0]	^{129}Xe	1/2	−0.777976	0	3.603[2]	3.588[2]
^{45}Sc	7/2	4.756487	−0.22	1.740[1]	1.737[1]	1.783[1]	^{131}Xe	3/2	0.6915	−0.114	1.586[2]	1.581[2]
^{47}Ti	5/2	−0.78848	0.302	6.725[−1]	6.727[−1]	6.896[−1]	^{133}Cs	7/2	2.582025	−0.00343	1.967[3]	1.958[3]
^{49}Ti	7/2	−1.10417	0.247	1.211[0]	1.212[0]	1.242[0]	^{135}Ba	3/2	0.83794	0.16	3.088[2]	3.079[2]
^{51}V	7/2	5.148706	−0.043	3.370[1]	3.379[1]		^{137}Ba	3/2	0.93737	0.245	3.865[2]	3.847[2]
^{53}Cr	3/2	−0.47454	−0.15	4.698[−1]	4.657[−1]		^{139}La	7/2	2.783046	0.2	3.026[3]	3.010[3]
^{51}Mn	5/2	3.5683	0.41	2.804[1]	2.825[1]		^{141}Ce	7/2	1.09	0	5.336[2]	
^{55}Mn	5/2	3.4532	0.33	2.626[1]	2.670[1]		^{141}Pr	5/2	4.2754	−0.077	1.031[4]	1.025[4]
^{57}Fe	1/2	0.09044	0	4.806[−2]	4.783[−2]		^{143}Nd	7/2	−1.065	−0.61	6.733[2]	6.685[2]
^{59}Co	7/2	4.627	0.42	6.678[1]	6.522[1]		^{145}Nd	7/2	−0.656	−0.314	2.555[2]	2.537[2]
^{61}Ni	3/2	−0.75002	0.162	2.795[0]	2.698[0]		^{145}Pm	5/2	3.8	0.23	1.077[4]	3.505[2]
^{63}Cu	3/2	2.2236	−0.211	3.005[1]	2.963[1]		^{149}Sm	7/2	−0.6677	0.078	3.494[2]	4.517[3]
^{65}Cu	3/2	2.3817	−0.204	3.447[1]	3.388[1]		^{151}Eu	5/2	3.4717	0.83	1.187[4]	1.176[4]
^{67}Zn	5/2	0.875479	0.15	4.754[0]	4.732[0]		^{153}Eu	5/2	1.5324	2.22	2.308[3]	2.289[3]
^{69}Ga	3/2	2.01659	0.171	3.633[1]	3.620[1]		^{155}Gd	3/2	−0.2572	1.27	8.871[1]	8.848[1]
^{71}Ga	3/2	2.56227	0.107	5.867[1]	5.845[1]		^{157}Gd	3/2	−0.3398	1.36	1.548[2]	1.523[2]
^{73}Ge	9/2	−0.879468	−0.196	6.095[0]	6.072[0]		^{159}Tb	3/2	2.014	1.432	6.278[3]	6.212[3]
^{75}As	3/2	1.43948	0.314	2.671[1]	2.661[1]		^{161}Dy	5/2	−0.48	2.51	3.429[2]	3.397[2]
^{77}Se	1/2	0.535042	0	7.931[0]	7.902[0]		^{163}Dy	5/2	0.673	2.318	6.748[2]	6.667[2]
^{79}Br	3/2	2.1064	0.313	8.129[1]	8.099[1]		^{165}Ho	7/2	4.17	3.58	2.750[4]	2.710[4]
^{81}Br	3/2	2.270562	0.262	9.446[1]	9.411[1]		^{167}Er	7/2	−0.56385	3.57	5.746[2]	5.669[2]
^{83}Kr	9/2	−0.970669	0.259	1.499[1]	1.494[1]		^{169}Tm	1/2	−0.231	0	2.583[2]	2.559[2]
^{85}Rb	5/2	1.35298	0.276	3.948[1]	3.935[1]		^{171}Yb	1/2	0.49367	0	1.362[3]	1.341[3]
^{87}Sr	9/2	−1.0928	0.305	2.650[1]	2.643[1]		^{173}Yb	5/2	−0.648	2.8	1.091[3]	1.182[3]
^{89}Y	1/2	−0.137415	0	1.209[0]	1.205[0]		^{175}Lu	7/2	2.2323	3.49	1.372[4]	1.356[4]
^{91}Zr	5/2	−1.30362	−0.176	5.962[1]	5.934[1]		^{177}Hf	7/2	0.7935	3.37	1.989[3]	1.954[3]
^{93}Nb	9/2	6.1705	−0.32	1.367[3]	1.361[3]		^{179}Hf	9/2	−0.6409	3.79	1.232[3]	1.210[3]
^{95}Mo	5/2	−0.9142	−0.022	4.009[1]	3.992[1]		^{181}Ta	7/2	2.3705	3.17	2.049[4]	2.008[4]
^{97}Mo	5/2	−0.9335	0.255	4.180[1]	4.162[1]							

TABLE IV. Magnetic dipole transition rates A_{M1} and hyperfine-induced $2p^5 3s\ ^3P_0 \rightarrow 2p^6\ ^1S_0$ transition rates A_{HIT} in the absence of an external magnetic field for Ne-like ions ($11 \leqslant Z \leqslant 35$) from this work and other works. Nuclear magnetic moments μ_I are from [56]. All transition rates are given in s^{-1} and $a[b]$ represent $a \times 10^b$.

				A_{M1}		MCDHF-A_{M1} [20]				
Ions	I	μ	Q	*ab initio*	Rescaled	*ab initio*	Rescaled	A_{E2}	A_{HIT}	MCDHF-A_{HIT} [20]
^{23}Na	3/2	2.217522	0.104	1.415[−2]	1.070[−2]	1.0718[−2]	1.068[−2]	4.559[−8]	2.701[1]	2.6551[1]
^{25}Mg	5/2	−0.85545	0.199	5.580[−2]	4.878[−2]	4.8561[−2]	4.871[−2]	2.472[−7]	6.295[0]	6.2049[0]
^{27}Al	5/2	3.641507	0.1466	2.135[−1]	2.004[−1]	1.9915[−1]	2.001[−2]	1.288[−6]	2.080[2]	2.0598[2]
^{29}Si	1/2	−0.55529	0	7.628[−1]	7.434[−1]	7.3740[−1]	7.422[−1]	6.100[−6]	1.833[1]	1.8136[1]
^{31}P	1/2	1.1316	0	2.519[0]	2.504[0]	2.4815[0]	2.500[0]	2.577[−5]	1.298[2]	1.2833[2]
^{33}S	3/2	0.643821	−0.0678	7.671[0]	7.748[0]	7.6314[0]	7.686[0]	9.754[−5]	3.849[1]	3.8040[1]
^{35}Cl	3/2	0.821874	−0.817	2.154[1]	2.168[1]	2.1549[1]	2.162[0]	3.347[−4]	1.004[2]	9.9200[1]
^{37}Cl	3/2	0.684124	−0.0644						6.957[1]	6.8734[1]
^{39}K	3/2	0.39147	0.0585	1.356[2]	1.408[2]	1.3619[2]	1.404[2]	3.071[−3]	5.405[1]	5.3439[1]
^{41}K	3/2	0.21487	0.0711						1.628[1]	1.6099[1]
^{43}Ca	7/2	−1.3173	−0.04	3.078[2]		3.0937[2]		8.377[−3]	7.036[2]	6.9692[2]
^{45}Sc	7/2	4.756487	−0.22	6.601[2]	6.590[2]	6.6369[2]	6.575[2]	2.154[−2]	1.343[4]	1.3301[4]
^{47}Ti	5/2	−0.78848	0.302	1.347[3]	1.376[3]	1.3543[3]	1.373[3]	5.258[−2]	5.777[2]	5.7333[2]
^{49}Ti	7/2	−1.10417	0.247						1.040[3]	1.0325[3]
^{51}V	7/2	5.148706	−0.043	2.631[3]		2.6455[3]		1.224[−1]	3.210[4]	3.1868[4]
^{53}Cr	3/2	−0.47454	−0.15	4.947[3]	4.826[3]	4.9730[3]	4.818[3]	2.733[−1]	4.939[2]	4.9131[2]
^{51}Mn	5/2	3.5683	0.41	8.990[3]		9.0365[3]		5.872[−1]	3.242[4]	3.2271[4]
^{55}Mn	5/2	3.4532	0.33						3.037[4]	3.0495[4]
^{57}Fe	1/2	0.09044	0	1.585[4]	1.580[4]	1.5933[4]	1.593[4]	1.219[0]	6.097[1]	6.1188[1]
^{59}Co	7/2	4.627	0.42	2.721[4]		2.7346[4]		2.451[0]	9.261[4]	9.2257[4]
^{61}Ni	3/2	−0.75002	0.162	4.559[4]		4.5808[4]		4.787[0]	4.219[3]	4.2145[3]
^{63}Cu	3/2	2.2236	−0.211	7.472[4]		7.5066[4]		9.104[0]	4.940[4]	4.9424[4]
^{65}Cu	3/2	2.3817	−0.204						5.668[4]	5.6518[4]
^{67}Zn	5/2	0.875479	0.15	1.200[5]		1.2057[5]		1.689[1]	8.472[3]	8.4632[3]
^{69}Ga	3/2	2.01659	0.171	1.893[5]		1.9015[5]		3.063[1]	7.023[4]	7.0096[4]
^{71}Ga	3/2	2.56227	0.107						1.134[5]	1.1316[5]
^{73}Ge	9/2	−0.879468	−0.196	2.936[5]		2.9487[5]		5.436[1]	1.273[4]	1.2736[4]
^{75}As	3/2	1.43948	0.314	4.483[5]		4.5023[5]		9.459[1]	6.026[4]	6.0239[4]
^{77}Se	1/2	0.535042	0	6.747[5]		6.7763[5]		1.615[2]	1.931[4]	1.9298[4]
^{79}Br	3/2	2.1064	0.313	1.002[6]		1.0064[6]		2.709[2]	2.132[5]	2.1305[5]
^{81}Br	3/2	2.270562	0.262						2.477[5]	2.4755[5]

B. HIT

In Tables III and IV we present the resulting HIT transition rates, in the absence of an external magnetic field, for the two isoelectronic sequences. In the Be-like case, we give results in the range from B^+ to Ta^{69+}. The results are compared with the theoretical results by Cheng *et al.* [39] who performed calculations using relativistic configuration interaction and a radiation damping method, including experimental energies from the NIST Atomic Spectra Database (version 3.1.5) [55]. Comparing this with the present results, we find agreement to within 1%–2% for most of the isotopes in the isoelectronic sequence, with just a few exceptions. First, the disagreements for ^{103}Rh and ^{173}Yb are caused by the use of different nuclear magnetic moments μ_I. In the present calculations we use values from the most recent table [56]. If the earlier results are rescaled with the new μ_I values, the transition rates agree to within 0.19% and 1.26% for ^{103}Rh and ^{173}Yb, respectively. The differences for ^{59}Co, ^{61}Ni, and ^{181}Ta of 2.39%, 3.59%, and 2.05%, respectively, have no apparent explanation. We also compare our results with MCHDF calculations by Andersson *et al.* [16], when available. They present calculations for Be-like ions from C^{2+} to Ti^{18+}, to a somewhat lower accuracy than in this work. The *rescaled* results from the earlier work, corrected by the experimental energy values, agree with the present to within 1% for all isotopes.

In Table IV we present the results for the hyperfine-induced $2p^5 3s\ ^3P_0 \rightarrow 2p^6\ ^1S_0$ transition rates A_{HIT} in the absence of an external magnetic field for Ne-like ions, ranging from Na^+ to Br^{25+}. In a recent paper, Andersson *et al.* [20] analyzed the competition between forbidden and hyperfine-induced transitions in Ne-like ions using the MCDHF method. The present A_{M1} values, rescaled to experimental energies, are in

excellent agreement with their values. There is also general agreement for the $A_{\rm HIT}$ values along the sequence. The difference for $A_{\rm HIT}$ values are between 1% and 2% for the isotopes in the lower end of the isoelectronic sequence, while for higher Z it is less than 1%. This is due to the dependence on correlation effects for the transition rate $A_{\rm HIT}$. In this work, we include core-core interaction with the $2s$ subshell, in addition to valence-valence and core-valence interaction included also in Ref. [20]. In the RCI calculation, more CSFs are generated by SDT excitations to the smaller $n = 4$ orbital basis. As shown in Ref. [53], there is an almost perfect agreement between our excitation energies and experimental values to within less than 0.011% for the lowest ions in the sequence. As the atomic number Z increases, electron correlation effects decrease and the agreement between our $A_{\rm HIT}$ values and the ones provided by Andersson *et al.* [20] is better.

C. Measurements of HITs in the presence of magnetic fields in Be-like ions

Table V compares the theoretical $2s2p\,^3P_0 \rightarrow 2s^2\,^1S_0$ transition rate for Be-like ions to available experimental values. The experimental value for $^{15}N^{3+}$ was obtained from spectroscopic observations of the planetary nebula NGC3981 using the STIS instrument on the Hubble Space Telescope [33]. The resulting rate agrees with the presented theoretical results, but with fairly large uncertainties.

TABLE V. Comparison of experimental and theoretical values for the hyperfine-induced $2s2p\,^3P_0 \rightarrow 2s^2\,^1S_0$ transition rate in Be-like ions. All transition rates are given in s^{-1} and $a[b]$ represent $a \times 10^b$.

Ions	Reference	Values
$^{15}N^{3+}$		
$I = 1/2$	MCHF[a]	3.62[−4]
$\mu_I = -0.283189$	CI[b]	3.269[−4]
$Q = 0$	MCDHF[c]	3.285[−4]
	MCDHF[d]	4.40[−4]
	This work ($B = 0$)	3.271[−4]
	Space[e]	4.0 ± 1.3[−4]
$^{33}S^{12+}$		
$I = 3/2$	CI[b]	9.315[−2]
$\mu_I = 0.643821$	MCDHF[c]	9.439[−2]
$Q = -0.0678$	This work (HIT)	9.342[−2]
	This work (MIT-hfs at 0.444 T)	8.307[−2]
	This work ($A_{\rm avg}$ at 0.444 T)	9.208[−2]
	This work (MIT-hfs at 0.883 T)	7.583[−2]
	This work ($A_{\rm avg}$ at 0.883 T)	9.113[−2]
	Storage ring[f]	9.6 ± 0.4[−2]
$^{47}Ti^{18+}$		
$I = 5/2$	CI[b]	6.727[−1]
$\mu_I = -0.78848$	MCDHF[c]	6.896[−1]
$Q = 0.302$	MCDHF[d]	6.80[−1]
	This work (HIT)	6.725[−1]
	MCDHF[g] (MIT-hfs at 0.742 T)	6.65[−1]
	This work (MIT-hfs at 0.742 T)	6.895[−1]
	This work ($A_{\rm avg}$ at 0.742 T)	6.747[−1]
	Storage ring[h]	5.6 ± 0.3[−1]

[a]Brage *et al.* [3].
[b]Cheng *et al.* [39].
[c]Andersson *et al.* [16].
[d]Li and Dong [57].
[e]Brage *et al.* [33].
[f]Schippers *et al.* [34].
[g]Li *et al.* [37].
[h]Schippers *et al.* [35].

The experiment for $^{33}S^{12+}$ was carried out by employing the heavy-ion storage ring TSR [34]. The observed transition rate is $(9.6 \pm 0.4) \times 10^{-2}$ s^{-1} which agrees with the recent theoretical HIT value. The effect of external magnetic fields on the HIT rates has also been investigated experimentally by varying the magnetic-field strength of the storage ring dipoles by a factor of 2. It yields the same result under the different experimental conditions and it was concluded that within the experimental uncertainties, no significant influence of the magnetic field in the storage-ring bending magnets on the measured HIT transition rate was found. To compare with the experimental results, we present the MIT-hfs rates for ^{33}S at the magnetic-field strength of 0.444 and 0.883 T adopted in Ref. [34] in Table V. There is a ∼9% difference between the two different conditions and the absolute transition values differ by 13.4% and 21% with the experimental values, respectively. Considering the particular case that dipole bending magnets cover only part of the closed orbit of the stored ions in TSR, the average transition rate can be defined as

$$A_{\rm avg} = f_B A_{\text{MIT-hfs}}(B) + (1 - f_B) A_{\rm HIT}, \tag{23}$$

where f_B is the fraction of time spent in the magnetic field B, which is 13% in the case of ^{33}S. The difference of the $A_{\rm avg}$ values between the two magnetic-field conditions is ∼1.2% which can be ignored compared with the 4% experimental uncertainty. However, the MIT-hfs values still differ from the experimental ones by ∼6.5%.

As shown in Table V, there is a significant disagreement (23% to 36%) between the experimental and theoretical HIT results for Be-like ^{47}Ti. By considering the effect of the magnetic field, the MIT-hfs values and $A_{\rm avg}$ values at $B = 0.742$ T are listed in Table V. With the experimental uncertainty 5.4%, the disagreement can not be explained by the inclusion of MIT effect. As discussed in Ref. [42], there were no significant disturbances of the experimental results by external electric fields or by the E1M1 two-photon transition.

TABLE VI. Magnetic-field- and hyperfine-induced $2s2p\,^3P_0 \rightarrow 2s^2\,^1S_0$ transition rate $A_{\text{MIT-hfs}}$, in the presence of external magnetic field $B = 0.742$ T for Be-like ^{47}Ti with nuclear spin $I = \frac{5}{2}$. The $A_{\text{MIT-hfs}}$ (s^{-1}) were obtained by the inclusion of only the perturbers with $\Delta F = 0$ and of perturbers with $\Delta F = 0, \pm 1$. The results from [37] are shown in the last column. All transition rates are given in s^{-1} and $a[b]$ represent $a \times 10^b$.

	$A_{\text{MIT-hfs}}$		
M_F	$\Delta F = 0$	$\Delta F = 0, \pm 1$	$\Delta F = 0$ [37]
5/2	5.880[−1]	6.348[−1]	5.9[−1]
3/2	6.174[−1]	6.328[−1]	6.2[−1]
1/2	6.475[−1]	6.587[−1]	6.5[−1]
–1/2	6.783[−1]	6.897[−1]	6.8[−1]
–3/2	7.098[−1]	7.263[−1]	7.1[−1]
–5/2	7.420[−1]	7.945[−1]	7.4[−1]

Reference [37] discusses the possible nonstatistical population of the magnetic sublevels and concludes that this can not contribute to such a big difference. So, the reason for the discrepancy between experimental and theoretical HIT rates is still unclear. This indicates that further experimental studies would be important for comparison with the quite extensive calculations now available.

In Table VI we show the results for the magnetic-field- and hyperfine-induced $2s2p\,^3P_0 \rightarrow 2s^2\,^1S_0$ transition rate $A_{\text{MIT-hfs}}$

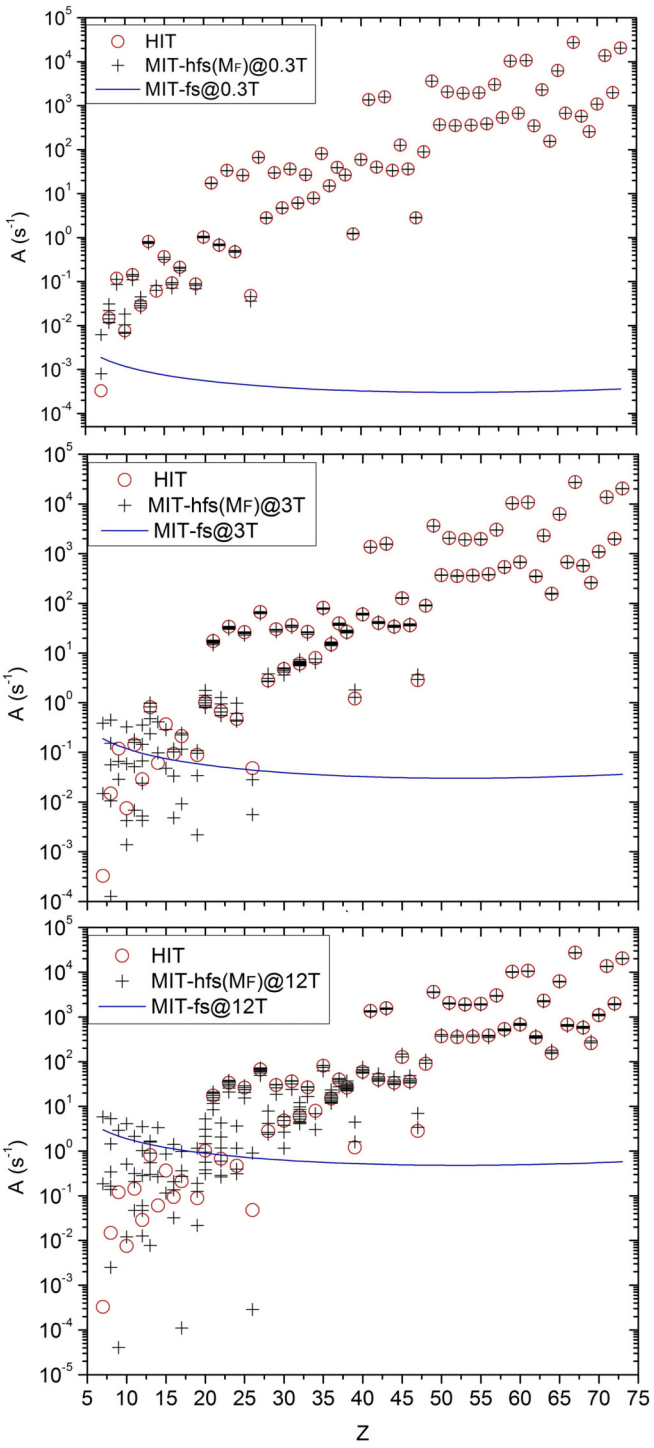

FIG. 3. Transition rates of $2s2p\,^3P_0$ associated with different transition channels to $2s^2\,^1S_0$ ground state in Be-like ions ($7 \leqslant Z \leqslant 73$). The MIT-fs and MIT-hfs values are given in the magnetic field of 0.3 T (upper panel), 3 T (middle panel), and 12 T (lower panel). The y axis is given in logarithmic scale.

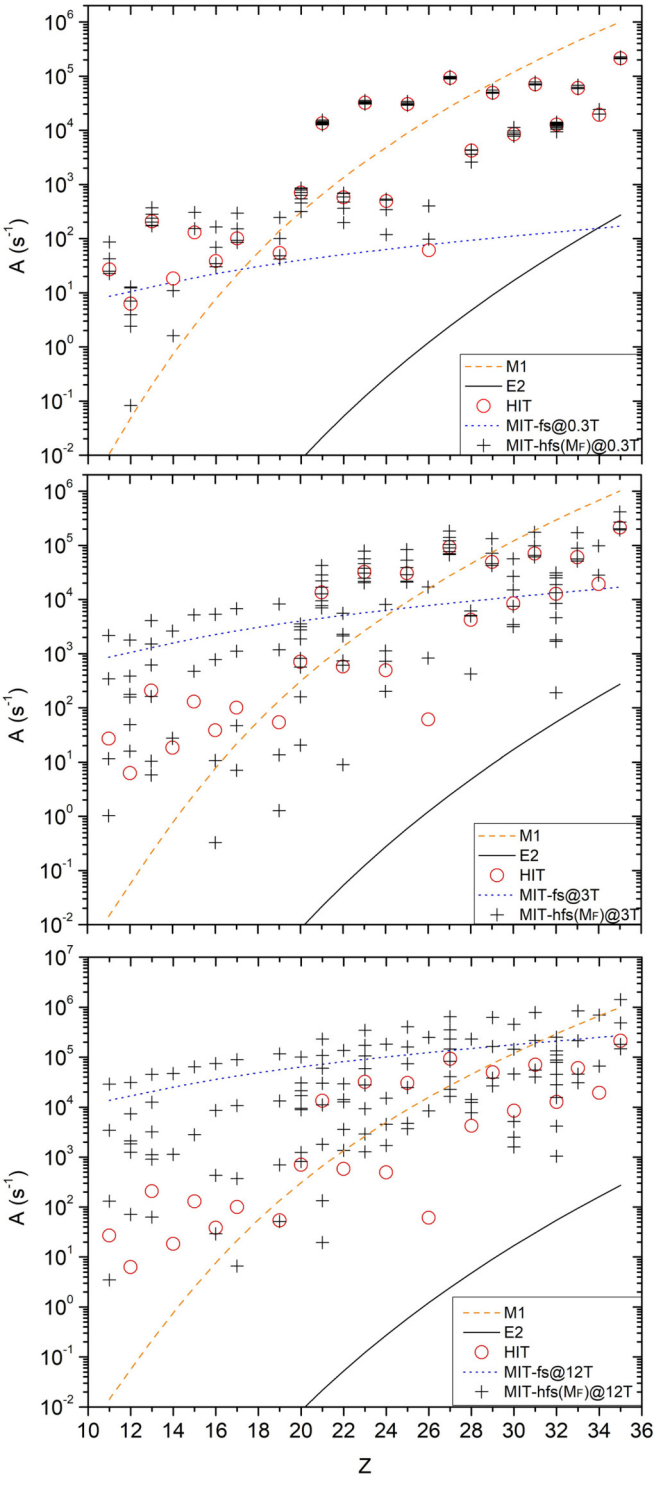

FIG. 4. Transition rates of $2p^5 3s\,^3P_0$ associated with different transition channels to lower states in Ne-like ions ($11 \leqslant Z \leqslant 35$). The MIT-fs and MIT-hfs values are given in the magnetic field of 0.3 T (upper panel), 3 T (middle panel), and 12 T (lower panel). The electric quadrupole (E2) transitions are ignored for the ions with the rates smaller than 10^{-2} s^{-1}. The y axis is given in logarithmic scale.

TABLE VII. Magnetic-field- and hyperfine-induced $2s2p\ ^3P_0 \rightarrow 2s^2\ ^1S_0$ transition rates $A_{\text{MIT-hfs}}$ for some Be-like ions with nuclear spin and with external magnetic fields of different strengths. All transition rates are given in s^{-1} and $a[b]$ represent $a \times 10^b$.

	$A_{\text{MIT-hfs}}$ (s^{-1})						
M_F	0.05 T	0.1 T	0.2 T	0.4 T	0.6 T	0.8 T	1 T
$Z = 5$, ^{11}B, $I = 3/2$, $\mu_I = 2.688649$, $Q = 0.04059$							
1.5	2.486[−3]	2.629[−3]	2.928[−3]	3.572[−3]	4.277[−3]	5.043[−3]	5.865[−3]
0.5	2.405[−3]	2.465[−3]	2.587[−3]	2.838[−3]	3.100[−3]	3.373[−3]	3.654[−3]
–0.5	1.925[−3]	1.546[−3]	9.118[−4]	1.433[−4]	3.858[−5]	5.920[−4]	1.795[−3]
–1.5	1.180[−3]	4.110[−4]	6.230[−5]	4.122[−3]	1.450[−2]	3.113[−2]	5.394[−2]
$Z = 6$, ^{13}C, $I = 1/2$, $\mu_I = 0.702412$, $Q = 0$							
0.5	7.1328[−4]	6.1237[−4]	4.3363[−4]	1.6848[−4]	2.6396[−5]	7.3037[−6]	1.1109[−4]
–0.5	2.9655[−4]	3.3322[−5]	2.9321[−4]	3.9580[−3]	1.1815[−2]	2.3860[−2]	4.0090[−2]
$Z = 7$, ^{15}N, $I = 1/2$, $\mu_I = -0.283189$, $Q = 0$							
0.5	3.871[−4]	4.580[−4]	6.177[−4]	1.009[−3]	1.495[−3]	2.076[−3]	2.753[−3]
–0.5	7.841[−4]	1.448[−3]	3.383[−3]	9.678[−3]	1.921[−2]	3.197[−2]	4.796[−2]
$Z = 9$, ^{19}F, $I = 1/2$, $\mu_I = 2.628868$, $Q = 0.0942$							
0.5	1.168[−1]	1.158[−1]	1.138[−1]	1.099[−1]	1.061[−1]	1.023[−1]	9.863[−2]
–0.5	1.120[−1]	1.063[−1]	9.551[−2]	7.557[−2]	5.797[−2]	4.269[−2]	2.975[−2]
$Z = 10$, ^{21}Ne, $I = 3/2$, $\mu_I = -0.661797$, $Q = 0.102$							
1.5	7.258[−3]	7.120[−3]	6.847[−3]	6.319[−3]	5.811[−3]	5.325[−3]	4.860[−3]
0.5	7.338[−3]	7.278[−3]	7.160[−3]	6.926[−3]	6.696[−3]	6.470[−3]	6.248[−3]
–0.5	7.854[−3]	8.325[−3]	9.306[−3]	1.143[−2]	1.378[−2]	1.635[−2]	1.913[−2]
–1.5	8.852[−3]	1.044[−2]	1.400[−2]	2.268[−2]	3.346[−2]	4.632[−2]	6.126[−2]
$Z = 11$, ^{23}Na, $I = 3/2$, $\mu_I = 2.217522$, $Q = 0.104$							
1.5	1.416[−1]	1.422[−1]	1.433[−1]	1.457[−1]	1.481[−1]	1.504[−1]	1.529[−1]
0.5	1.413[−1]	1.415[−1]	1.420[−1]	1.430[−1]	1.440[−1]	1.451[−1]	1.461[−1]
–0.5	1.392[−1]	1.373[−1]	1.337[−1]	1.266[−1]	1.196[−1]	1.129[−1]	1.064[−1]
–1.5	1.353[−1]	1.298[−1]	1.190[−1]	9.887[−2]	8.061[−2]	6.420[−2]	4.966[−2]
$Z = 13$, ^{27}Al, $I = 5/2$, $\mu_I = 3.641507$, $Q = 0.1466$							
2.5	8.010[−1]	8.037[−1]	8.092[−1]	8.203[−1]	8.315[−1]	8.427[−1]	8.540[−1]
1.5	8.012[−1]	8.041[−1]	8.101[−1]	8.220[−1]	8.340[−1]	8.461[−1]	8.583[−1]
0.5	7.986[−1]	7.990[−1]	7.999[−1]	8.015[−1]	8.032[−1]	8.048[−1]	8.065[−1]
–0.5	7.957[−1]	7.931[−1]	7.880[−1]	7.778[−1]	7.677[−1]	7.576[−1]	7.476[−1]
–1.5	7.923[−1]	7.863[−1]	7.744[−1]	7.510[−1]	7.279[−1]	7.052[−1]	6.828[−1]
–2.5	7.861[−1]	7.741[−1]	7.503[−1]	7.039[−1]	6.590[−1]	6.155[−1]	5.735[−1]
$Z = 16$, ^{33}S, $I = 3/2$, $\mu_I = 0.643821$, $Q = -0.0678$							
1.5	9.247[−2]	9.286[−2]	9.362[−2]	9.517[−2]	9.672[−2]	9.829[−2]	9.987[−2]
0.5	9.226[−2]	9.242[−2]	9.275[−2]	9.341[−2]	9.407[−2]	9.473[−2]	9.540[−2]
–0.5	9.088[−2]	8.967[−2]	8.728[−2]	8.259[−2]	7.804[−2]	7.361[−2]	6.931[−2]
–1.5	8.836[−2]	8.471[−2]	7.763[−2]	6.441[−2]	5.241[−2]	4.165[−2]	3.213[−2]
$Z = 17$, ^{35}Cl, $I = 3/2$, $\mu_I = 0.821874$, $Q = -0.817$							
1.5	2.094[−1]	2.099[−1]	2.111[−1]	2.133[−1]	2.156[−1]	2.178[−1]	2.201[−1]
0.5	2.091[−1]	2.093[−1]	2.098[−1]	2.107[−1]	2.117[−1]	2.127[−1]	2.136[−1]
–0.5	2.071[−1]	2.053[−1]	2.018[−1]	1.948[−1]	1.880[−1]	1.813[−1]	1.748[−1]
–1.5	2.034[−1]	1.980[−1]	1.874[−1]	1.671[−1]	1.480[−1]	1.301[−1]	1.133[−1]
$Z = 17$, ^{37}Cl, $I = 3/2$, $\mu_I = 0.684124$, $Q = -0.0644$							
1.5	1.452[−1]	1.456[−1]	1.465[−1]	1.484[−1]	1.503[−1]	1.522[−1]	1.541[−1]
0.5	1.449[−1]	1.451[−1]	1.455[−1]	1.463[−1]	1.471[−1]	1.479[−1]	1.487[−1]
–0.5	1.432[−1]	1.417[−1]	1.388[−1]	1.331[−1]	1.274[−1]	1.220[−1]	1.166[−1]
–1.5	1.401[−1]	1.357[−1]	1.270[−1]	1.104[−1]	9.495[−2]	8.069[−2]	6.759[−2]
$Z = 19$, ^{39}K, $I = 3/2$, $\mu_I = 0.39147$, $Q = 0.0585$							
1.5	8.729[−2]	8.763[−2]	8.832[−2]	8.969[−2]	9.107[−2]	9.247[−2]	9.387[−2]
0.5	8.710[−2]	8.725[−2]	8.754[−2]	8.812[−2]	8.871[−2]	8.930[−2]	8.989[−2]
–0.5	8.587[−2]	8.479[−2]	8.266[−2]	7.848[−2]	7.440[−2]	7.044[−2]	6.658[−2]
–1.5	8.363[−2]	8.037[−2]	7.404[−2]	6.217[−2]	5.133[−2]	4.153[−2]	3.277[−2]

TABLE VII. (*Continued.*)

	$A_{\text{MIT-hfs}}$ (s^{-1})						
M_F	0.05 T	0.1 T	0.2 T	0.4 T	0.6 T	0.8 T	1 T
$Z = 19$, ^{41}K, $I = 3/2$, $\mu_I = 0.21487$, $Q = 0.0711$							
1.5	2.638[–2]	2.657[–2]	2.694[–2]	2.771[–2]	2.848[–2]	2.926[–2]	3.005[–2]
0.5	2.627[–2]	2.635[–2]	2.651[–2]	2.684[–2]	2.716[–2]	2.749[–2]	2.782[–2]
–0.5	2.560[–2]	2.502[–2]	2.386[–2]	2.164[–2]	1.953[–2]	1.752[–2]	1.562[–2]
–1.5	2.438[–2]	2.264[–2]	1.934[–2]	1.353[–2]	8.749[–3]	5.008[–3]	2.304[–3]
$Z = 20$, ^{43}Ca, $I = 7/2$, $\mu_I = -1.3173$, $Q = -0.0408$							
3.5	1.002[0]	9.992[–1]	9.927[–1]	9.799[–1]	9.671[–1]	9.544[–1]	9.418[–1]
2.5	1.002[0]	9.982[–1]	9.909[–1]	9.762[–1]	9.616[–1]	9.472[–1]	9.328[–1]
1.5	1.004[0]	1.001[0]	9.972[–1]	9.887[–1]	9.803[–1]	9.720[–1]	9.636[–1]
0.5	1.005[0]	1.005[0]	1.005[0]	1.003[0]	1.002[0]	1.001[0]	1.000[0]
–0.5	1.007[0]	1.009[0]	1.012[0]	1.019[0]	1.026[0]	1.033[0]	1.040[0]
–1.5	1.010[0]	1.013[0]	1.021[0]	1.037[0]	1.052[0]	1.068[0]	1.084[0]
–2.5	1.012[0]	1.018[0]	1.031[0]	1.056[0]	1.082[0]	1.108[0]	1.135[0]
–3.5	1.016[0]	1.027[0]	1.049[0]	1.093[0]	1.138[0]	1.184[0]	1.231[0]
$Z = 22$, ^{47}Ti, $I = 5/2$, $\mu_I = -0.78848$, $Q = 0.302$							
2.5	6.609[–1]	6.590[–1]	6.552[–1]	6.476[–1]	6.401[–1]	6.326[–1]	6.252[–1]
1.5	6.608[–1]	6.587[–1]	6.546[–1]	6.465[–1]	6.385[–1]	6.305[–1]	6.225[–1]
0.5	6.625[–1]	6.622[–1]	6.617[–1]	6.606[–1]	6.595[–1]	6.583[–1]	6.572[–1]
–0.5	6.646[–1]	6.664[–1]	6.700[–1]	6.772[–1]	6.845[–1]	6.919[–1]	6.992[–1]
–1.5	6.670[–1]	6.712[–1]	6.796[–1]	6.967[–1]	7.139[–1]	7.314[–1]	7.490[–1]
–2.5	6.713[–1]	6.798[–1]	6.971[–1]	7.323[–1]	7.684[–1]	8.053[–1]	8.431[–1]
$Z = 22$, ^{49}Ti, $I = 7/2$, $\mu_I = -1.10417$, $Q = 0.247$							
3.5	1.190[0]	1.187[0]	1.180[0]	1.167[0]	1.153[0]	1.140[0]	1.127[0]
2.5	1.190[0]	1.186[0]	1.178[0]	1.163[0]	1.148[0]	1.133[0]	1.118[0]
1.5	1.192[0]	1.189[0]	1.185[0]	1.176[0]	1.167[0]	1.159[0]	1.150[0]
0.5	1.193[0]	1.193[0]	1.192[0]	1.191[0]	1.190[0]	1.189[0]	1.188[0]
–0.5	1.196[0]	1.197[0]	1.201[0]	1.208[0]	1.215[0]	1.222[0]	1.230[0]
–1.5	1.198[0]	1.202[0]	1.210[0]	1.226[0]	1.242[0]	1.259[0]	1.275[0]
–2.5	1.200[0]	1.207[0]	1.220[0]	1.246[0]	1.273[0]	1.300[0]	1.328[0]
–3.5	1.205[0]	1.216[0]	1.239[0]	1.285[0]	1.331[0]	1.379[0]	1.427[0]
$Z = 23$, ^{51}V$I = 7/2$, $\mu_I = 5.148706$, $Q = -0.043$							
3.5	3.324[1]	3.326[1]	3.329[1]	3.336[1]	3.343[1]	3.350[1]	3.357[1]
2.5	3.324[1]	3.326[1]	3.330[1]	3.338[1]	3.346[1]	3.354[1]	3.362[1]
1.5	3.324[1]	3.325[1]	3.327[1]	3.332[1]	3.336[1]	3.341[1]	3.345[1]
0.5	3.323[1]	3.323[1]	3.323[1]	3.324[1]	3.324[1]	3.325[1]	3.325[1]
–0.5	3.321[1]	3.321[1]	3.319[1]	3.315[1]	3.311[1]	3.308[1]	3.304[1]
–1.5	3.320[1]	3.318[1]	3.314[1]	3.306[1]	3.298[1]	3.289[1]	3.281[1]
–2.5	3.319[1]	3.316[1]	3.309[1]	3.296[1]	3.282[1]	3.269[1]	3.255[1]
–3.5	3.317[1]	3.311[1]	3.299[1]	3.276[1]	3.254[1]	3.231[1]	3.208[1]
$Z = 24$, ^{53}Cr, $I = 3/2$, $\mu_I = -0.47454$, $Q = -0.15$							
1.5	4.623[–1]	4.616[–1]	4.602[–1]	4.574[–1]	4.546[–1]	4.519[–1]	4.491[–1]
0.5	4.627[–1]	4.624[–1]	4.618[–1]	4.606[–1]	4.594[–1]	4.582[–1]	4.570[–1]
–0.5	4.653[–1]	4.675[–1]	4.721[–1]	4.812[–1]	4.904[–1]	4.997[–1]	5.090[–1]
–1.5	4.700[–1]	4.770[–1]	4.912[–1]	5.202[–1]	5.500[–1]	5.807[–1]	6.122[–1]
$Z = 25$, ^{51}Mn, $I = 5/2$, $\mu_I = 3.5683$, $Q = 0.41$							
2.5	2.766[1]	2.767[1]	2.769[1]	2.774[1]	2.779[1]	2.783[1]	2.788[1]
1.5	2.766[1]	2.767[1]	2.770[1]	2.775[1]	2.780[1]	2.785[1]	2.790[1]
0.5	2.765[1]	2.765[1]	2.765[1]	2.766[1]	2.767[1]	2.767[1]	2.768[1]
–0.5	2.764[1]	2.762[1]	2.760[1]	2.756[1]	2.752[1]	2.747[1]	2.743[1]
–1.5	2.762[1]	2.760[1]	2.754[1]	2.744[1]	2.734[1]	2.724[1]	2.714[1]
–2.5	2.759[1]	2.754[1]	2.744[1]	2.724[1]	2.703[1]	2.683[1]	2.662[1]
$Z = 25$, ^{55}Mn, $I = 5/2$, $\mu_I = 3.4532$, $Q = 0.33$							
2.5	2.590[1]	2.591[1]	2.594[1]	2.598[1]	2.603[1]	2.607[1]	2.612[1]
1.5	2.590[1]	2.591[1]	2.594[1]	2.599[1]	2.604[1]	2.608[1]	2.613[1]
0.5	2.589[1]	2.589[1]	2.590[1]	2.590[1]	2.591[1]	2.592[1]	2.592[1]

TABLE VII. (*Continued.*)

	$A_{\text{MIT-hfs}}$ (s^{-1})						
M_F	0.05 T	0.1 T	0.2 T	0.4 T	0.6 T	0.8 T	1 T
–0.5	2.588[1]	2.587[1]	2.585[1]	2.581[1]	2.576[1]	2.572[1]	2.568[1]
–1.5	2.587[1]	2.584[1]	2.579[1]	2.569[1]	2.560[1]	2.550[1]	2.540[1]
–2.5	2.584[1]	2.579[1]	2.569[1]	2.549[1]	2.530[1]	2.510[1]	2.490[1]
$Z = 26$, ^{57}Fe, $I = 1/2$, $\mu_I = 0.09044$, $Q = 0$							
0.5	4.701[–2]	4.664[–2]	4.592[–2]	4.450[–2]	4.310[–2]	4.172[–2]	4.037[–2]
–0.5	4.527[–2]	4.322[–2]	3.926[–2]	3.191[–2]	2.533[–2]	1.950[–2]	1.444[–2]

from each magnetic sublevel at $B = 0.742$ T for Be-like ^{47}Ti, both with the inclusion of only the "diagonal" $\Delta F = 0$ perturbers, as well as of also including the off-diagonal $\Delta F = \pm 1$ ones. This illustrates the difference between our present calculations and the earlier results from [37], shown in the last column, which only included the diagonal $\Delta F = 0$ perturbers. It is clear that the contribution from $\Delta F = \pm 1$ perturbers is significant for the MIT-hfs probabilities.

TABLE VIII. Magnetic-field- and hyperfine-induced $2p^5 3s\ ^3P_0 \rightarrow 2p^6\ ^1S_0$ transition rates $A_{\text{MIT-hfs}}$ for Ne-like ions ($11 \leqslant Z \leqslant 35$) with nuclear spin in a magnetic filed of different strengths. All transition rates are given in s^{-1} and $a[b]$ represent $a \times 10^b$.

	$A_{\text{MIT-hfs}}$ (s^{-1})						
M_F	0.05 T	0.1 T	0.2 T	0.4 T	0.6 T	0.8 T	1 T
$Z = 11$, ^{23}Na, $I = 3/2$, $\mu_I = 2.217522$, $Q = 0.104$							
1.5	2.591[1]	2.521[1]	2.384[1]	2.122[1]	1.875[1]	1.643[1]	1.426[1]
0.5	2.631[1]	2.602[1]	2.542[1]	2.425[1]	2.311[1]	2.200[1]	2.092[1]
–0.5	2.896[1]	3.141[1]	3.660[1]	4.818[1]	6.135[1]	7.610[1]	9.245[1]
–1.5	3.418[1]	4.268[1]	6.253[1]	1.135[2]	1.797[2]	2.609[2]	3.572[2]
$Z = 12$, ^{25}Mg, $I = 5/2$, $\mu_I = -0.85545$, $Q = 0.199$							
2.5	7.067[0]	7.987[0]	9.995[0]	1.468[1]	2.027[1]	2.676[1]	3.415[1]
1.5	7.133[0]	8.127[0]	1.031[1]	1.545[1]	2.163[1]	2.885[1]	3.710[1]
0.5	6.328[0]	6.453[0]	6.707[0]	7.229[0]	7.771[0]	8.332[0]	8.913[0]
–0.5	5.444[0]	4.733[0]	3.461[0]	1.512[0]	3.589[–1]	9.908[–4]	4.383[–1]
–1.5	4.510[0]	3.086[0]	1.045[0]	1.990[–1]	3.666[0]	1.145[1]	2.354[1]
–2.5	3.051[0]	1.005[0]	2.363[–1]	1.199[1]	4.147[1]	8.868[1]	1.536[2]
$Z = 13$, ^{27}Al, $I = 5/2$, $\mu_I = 3.641507$, $Q = 0.1466$							
2.5	1.998[2]	1.946[2]	1.844[2]	1.648[2]	1.463[2]	1.290[2]	1.127[2]
1.5	1.994[2]	1.938[2]	1.829[2]	1.621[2]	1.425[2]	1.241[2]	1.071[2]
0.5	2.043[2]	2.035[2]	2.020[2]	1.990[2]	1.960[2]	1.930[2]	1.901[2]
–0.5	2.101[2]	2.152[2]	2.256[2]	2.471[2]	2.696[2]	2.931[2]	3.176[2]
–1.5	2.168[2]	2.290[2]	2.543[2]	3.088[2]	3.687[2]	4.338[2]	5.043[2]
–2.5	2.293[2]	2.549[2]	3.103[2]	4.372[2]	5.859[2]	7.562[2]	9.483[2]
$Z = 14$, ^{29}Si, $I = 1/2$, $\mu_I = -0.55529$, $Q = 0$							
0.5	1.675[1]	1.548[1]	1.310[1]	8.933[0]	5.560[0]	2.983[0]	1.202[0]
–0.5	1.109[1]	5.814[0]	3.269[–1]	9.654[0]	4.605[1]	1.095[2]	2.000[2]
$Z = 15$, ^{31}P, $I = 1/2$, $\mu_I = 1.1316$, $Q = 0$							
0.5	1.319[2]	1.359[2]	1.441[2]	1.612[2]	1.793[2]	1.983[2]	2.183[2]
–0.5	1.518[2]	1.776[2]	2.355[2]	3.757[2]	5.486[2]	7.540[2]	9.920[2]
$Z = 16$, ^{33}S, $I = 3/2$, $\mu_I = 0.643821$, $Q = -0.0678$							
1.5	3.657[1]	3.522[1]	3.261[1]	2.768[1]	2.316[1]	1.905[1]	1.533[1]
0.5	3.735[1]	3.676[1]	3.560[1]	3.334[1]	3.116[1]	2.905[1]	2.701[1]
–0.5	4.249[1]	4.731[1]	5.772[1]	8.163[1]	1.097[2]	1.419[2]	1.782[2]
–1.5	5.285[1]	7.023[1]	1.124[2]	2.263[2]	3.797[2]	5.726[2]	8.049[2]
$Z = 17$, ^{35}Cl, $I = 3/2$, $\mu_I = 0.821874$, $Q = -0.817$							
1.5	9.656[1]	9.418[1]	8.952[1]	8.056[1]	7.206[1]	6.404[1]	5.649[1]
0.5	9.793[1]	9.690[1]	9.485[1]	9.083[1]	8.690[1]	8.306[1]	7.930[1]
–0.5	1.069[2]	1.151[2]	1.324[2]	1.706[2]	2.138[2]	2.617[2]	3.146[2]
–1.5	1.244[2]	1.526[2]	2.179[2]	3.831[2]	5.946[2]	8.525[2]	1.157[3]

TABLE VIII. *(Continued.)*

	$A_{\text{MIT-hfs}}$ (s^{-1})						
M_F	0.05 T	0.1 T	0.2 T	0.4 T	0.6 T	0.8 T	1 T
$Z = 17$, ^{37}Cl, $I = 3/2$, $\mu_I = 0.684124$, $Q = -0.0644$							
1.5	6.657[1]	6.460[1]	6.075[1]	5.341[1]	4.654[1]	4.014[1]	3.421[1]
0.5	6.771[1]	6.685[1]	6.516[1]	6.183[1]	5.859[1]	5.544[1]	5.238[1]
–0.5	7.517[1]	8.207[1]	9.679[1]	1.299[2]	1.678[2]	2.106[2]	2.582[2]
–1.5	8.994[1]	1.142[2]	1.714[2]	3.206[2]	5.161[2]	7.579[2]	1.046[3]
$Z = 19$, ^{39}K, $I = 3/2$, $\mu_I = 0.39147$, $Q = 0.0585$							
1.5	5.124[1]	4.925[1]	4.539[1]	3.814[1]	3.151[1]	2.552[1]	2.016[1]
0.5	5.240[1]	5.153[1]	4.981[1]	4.646[1]	4.324[1]	4.012[1]	3.713[1]
–0.5	6.004[1]	6.721[1]	8.277[1]	1.187[2]	1.612[2]	2.101[2]	2.655[2]
–1.5	7.549[1]	1.016[2]	1.653[2]	3.391[2]	5.747[2]	8.721[2]	1.231[3]
$Z = 19$, ^{41}K, $I = 3/2$, $\mu_I = 0.21487$, $Q = 0.0711$							
1.5	1.494[1]	1.388[1]	1.187[1]	8.311[0]	5.389[0]	3.097[0]	1.436[0]
0.5	1.557[1]	1.510[1]	1.418[1]	1.242[1]	1.078[1]	9.255[0]	7.847[0]
–0.5	1.986[1]	2.406[1]	3.370[1]	5.782[1]	8.841[1]	1.255[2]	1.690[2]
–1.5	2.911[1]	4.604[1]	9.147[1]	2.287[2]	4.277[2]	6.885[2]	1.011[3]
$Z = 20$, ^{43}Ca, $I = 7/2$, $\mu_I = -1.3173$, $Q = -0.04$							
3.5	7.165[2]	7.398[2]	7.876[2]	8.877[2]	9.938[2]	1.106[3]	1.224[3]
2.5	7.198[2]	7.465[2]	8.015[2]	9.174[2]	1.041[3]	1.173[3]	1.312[3]
1.5	7.085[2]	7.236[2]	7.543[2]	8.177[2]	8.836[2]	9.521[2]	1.023[3]
0.5	6.954[2]	6.974[2]	7.013[2]	7.091[2]	7.170[2]	7.249[2]	7.328[2]
–0.5	6.815[2]	6.696[2]	6.461[2]	6.004[2]	5.564[2]	5.141[2]	4.734[2]
–1.5	6.667[2]	6.404[2]	5.894[2]	4.938[2]	4.066[2]	3.279[2]	2.576[2]
–2.5	6.503[2]	6.085[2]	5.290[2]	3.867[2]	2.667[2]	1.689[2]	9.331[1]
–3.5	6.204[2]	5.513[2]	4.255[2]	2.226[2]	8.489[1]	1.230[1]	4.841[0]
$Z = 21$, ^{45}Sc, $I = 7/2$, $\mu_I = 4.756487$, $Q = -0.22$							
3.5	1.313[4]	1.303[4]	1.282[4]	1.240[4]	1.200[4]	1.160[4]	1.120[4]
2.5	1.312[4]	1.300[4]	1.276[4]	1.229[4]	1.182[4]	1.137[4]	1.092[4]
1.5	1.317[4]	1.310[4]	1.296[4]	1.269[4]	1.242[4]	1.215[4]	1.188[4]
0.5	1.323[4]	1.322[4]	1.320[4]	1.316[4]	1.313[4]	1.309[4]	1.305[4]
–0.5	1.329[4]	1.335[4]	1.346[4]	1.369[4]	1.391[4]	1.414[4]	1.437[4]
–1.5	1.337[4]	1.349[4]	1.375[4]	1.426[4]	1.479[4]	1.532[4]	1.587[4]
–2.5	1.344[4]	1.365[4]	1.407[4]	1.492[4]	1.580[4]	1.670[4]	1.763[4]
–3.5	1.359[4]	1.395[4]	1.467[4]	1.618[4]	1.776[4]	1.942[4]	2.114[4]
$Z = 22$, ^{47}Ti, $I = 5/2$, $\mu_I = -0.78848$, $Q = 0.302$							
2.5	5.872[2]	6.052[2]	6.420[2]	7.190[2]	8.003[2]	8.860[2]	9.760[2]
1.5	5.885[2]	6.078[2]	6.475[2]	7.306[2]	8.187[2]	9.118[2]	1.010[3]
0.5	5.720[2]	5.745[2]	5.797[2]	5.901[2]	6.006[2]	6.112[2]	6.218[2]
–0.5	5.529[2]	5.367[2]	5.049[2]	4.443[2]	3.876[2]	3.347[2]	2.857[2]
–1.5	5.314[2]	4.948[2]	4.254[2]	3.024[2]	2.003[2]	1.191[2]	5.895[1]
–2.5	4.939[2]	4.237[2]	2.994[2]	1.155[2]	1.754[1]	5.617[0]	7.971[1]
$Z = 22$, ^{49}Ti, $I = 7/2$, $\mu_I = -1.10417$, $Q = 0.247$							
3.5	1.057[3]	1.089[3]	1.154[3]	1.290[3]	1.435[3]	1.586[3]	1.745[3]
2.5	1.062[3]	1.098[3]	1.173[3]	1.331[3]	1.498[3]	1.676[3]	1.863[3]
1.5	1.046[3]	1.067[3]	1.109[3]	1.195[3]	1.285[3]	1.378[3]	1.474[3]
0.5	1.028[3]	1.031[3]	1.036[3]	1.047[3]	1.058[3]	1.068[3]	1.079[3]
–0.5	1.009[3]	9.927[2]	9.605[2]	8.976[2]	8.368[2]	7.781[2]	7.216[2]
–1.5	9.887[2]	9.526[2]	8.824[2]	7.500[2]	6.284[2]	5.175[2]	4.174[2]
–2.5	9.662[2]	9.086[2]	7.989[2]	6.005[2]	4.303[2]	2.885[2]	1.749[2]
–3.5	9.251[2]	8.298[2]	6.549[2]	3.670[2]	1.619[2]	3.959[1]	1.993[–2]
$Z = 23$, ^{51}V, $I = 7/2$, $\mu_I = 5.148706$, $Q = -0.043$							
3.5	3.145[4]	3.127[4]	3.091[4]	3.018[4]	2.947[4]	2.876[4]	2.807[4]
2.5	3.143[4]	3.122[4]	3.080[4]	2.998[4]	2.916[4]	2.836[4]	2.756[4]
1.5	3.152[4]	3.140[4]	3.116[4]	3.068[4]	3.020[4]	2.973[4]	2.926[4]
0.5	3.162[4]	3.160[4]	3.157[4]	3.150[4]	3.144[4]	3.137[4]	3.130[4]
–0.5	3.173[4]	3.183[4]	3.202[4]	3.241[4]	3.280[4]	3.319[4]	3.358[4]

TABLE VIII. *(Continued.)*

	$A_{\text{MIT-hfs}}$ (s^{-1})						
M_F	0.05 T	0.1 T	0.2 T	0.4 T	0.6 T	0.8 T	1 T
–1.5	3.186[4]	3.207[4]	3.251[4]	3.340[4]	3.429[4]	3.520[4]	3.612[4]
–2.5	3.199[4]	3.235[4]	3.306[4]	3.452[4]	3.601[4]	3.753[4]	3.908[4]
–3.5	3.225[4]	3.286[4]	3.410[4]	3.666[4]	3.931[4]	4.205[4]	4.489[4]
$Z = 24$, ^{53}Cr, $I = 3/2$, $\mu_I = -0.47454$, $Q = -0.15$							
1.5	4.951[2]	5.035[2]	5.205[2]	5.554[2]	5.915[2]	6.286[2]	6.669[2]
0.5	4.903[2]	4.939[2]	5.011[2]	5.155[2]	5.302[2]	5.451[2]	5.603[2]
–0.5	4.605[2]	4.349[2]	3.860[2]	2.969[2]	2.195[2]	1.538[2]	9.970[1]
–1.5	4.080[2]	3.361[2]	2.133[2]	5.107[1]	9.727[–2]	6.037[1]	2.319[2]
$Z = 25$, ^{51}Mn, $I = 5/2$, $\mu_I = 3.5683$, $Q = 0.41$							
2.5	3.180[4]	3.165[4]	3.134[4]	3.073[4]	3.012[4]	2.952[4]	2.892[4]
1.5	3.179[4]	3.162[4]	3.129[4]	3.063[4]	2.998[4]	2.933[4]	2.870[4]
0.5	3.193[4]	3.191[4]	3.186[4]	3.177[4]	3.167[4]	3.158[4]	3.148[4]
–0.5	3.210[4]	3.225[4]	3.254[4]	3.313[4]	3.372[4]	3.432[4]	3.492[4]
–1.5	3.230[4]	3.264[4]	3.333[4]	3.472[4]	3.615[4]	3.760[4]	3.909[4]
–2.5	3.265[4]	3.335[4]	3.477[4]	3.770[4]	4.074[4]	4.391[4]	4.719[4]
$Z = 25$, ^{55}Mn, $I = 5/2$, $\mu_I = 3.4532$, $Q = 0.33$							
2.5	2.978[4]	2.963[4]	2.933[4]	2.874[4]	2.815[4]	2.757[4]	2.699[4]
1.5	2.977[4]	2.961[4]	2.928[4]	2.865[4]	2.802[4]	2.739[4]	2.678[4]
0.5	2.990[4]	2.988[4]	2.984[4]	2.974[4]	2.965[4]	2.956[4]	2.947[4]
–0.5	3.007[4]	3.021[4]	3.049[4]	3.106[4]	3.163[4]	3.221[4]	3.280[4]
–1.5	3.026[4]	3.059[4]	3.125[4]	3.261[4]	3.399[4]	3.540[4]	3.684[4]
–2.5	3.060[4]	3.127[4]	3.265[4]	3.549[4]	3.845[4]	4.153[4]	4.472[4]
$Z = 26$, ^{57}Fe, $I = 1/2$, $\mu_I = 0.09044$, $Q = 0$							
0.5	6.564[1]	7.144[1]	8.377[1]	1.114[2]	1.429[2]	1.784[2]	2.178[2]
–0.5	9.592[1]	1.401[2]	2.535[2]	5.803[2]	1.041[3]	1.634[3]	2.362[3]
$Z = 27$, ^{59}Co, $I = 7/2$, $\mu_I = 4.627$, $Q = 0.42$							
3.5	9.089[4]	9.051[4]	8.975[4]	8.824[4]	8.674[4]	8.525[4]	8.378[4]
2.5	9.084[4]	9.040[4]	8.953[4]	8.780[4]	8.608[4]	8.439[4]	8.271[4]
1.5	9.102[4]	9.077[4]	9.027[4]	8.926[4]	8.827[4]	8.727[4]	8.629[4]
0.5	9.124[4]	9.120[4]	9.113[4]	9.098[4]	9.084[4]	9.069[4]	9.055[4]
–0.5	9.147[4]	9.167[4]	9.207[4]	9.286[4]	9.366[4]	9.447[4]	9.527[4]
–1.5	9.172[4]	9.217[4]	9.308[4]	9.491[4]	9.675[4]	9.861[4]	1.005[5]
–2.5	9.201[4]	9.274[4]	9.422[4]	9.722[4]	1.003[5]	1.034[5]	1.065[5]
–3.5	9.253[4]	9.380[4]	9.637[4]	1.016[5]	1.070[5]	1.125[5]	1.181[5]
$Z = 28$, ^{61}Ni, $I = 3/2$, $\mu_I = -0.75002$, $Q = 0.162$							
1.5	4.187[3]	4.217[3]	4.276[3]	4.396[3]	4.518[3]	4.641[3]	4.767[3]
0.5	4.170[3]	4.183[3]	4.208[3]	4.258[3]	4.309[3]	4.360[3]	4.411[3]
–0.5	4.064[3]	3.971[3]	3.788[3]	3.435[3]	3.099[3]	2.781[3]	2.480[3]
–1.5	3.871[3]	3.594[3]	3.072[3]	2.150[3]	1.392[3]	7.979[2]	3.682[2]
$Z = 29$, ^{63}Cu, $I = 3/2$, $\mu_I = 2.2236$, $Q = -0.211$							
1.5	4.859[4]	4.848[4]	4.827[4]	4.784[4]	4.742[4]	4.700[4]	4.658[4]
0.5	4.864[4]	4.860[4]	4.850[4]	4.831[4]	4.812[4]	4.794[4]	4.775[4]
–0.5	4.903[4]	4.937[4]	5.005[4]	5.142[4]	5.282[4]	5.423[4]	5.566[4]
–1.5	4.974[4]	5.080[4]	5.296[4]	5.741[4]	6.204[4]	6.685[4]	7.184[4]
$Z = 29$, ^{65}Cu, $I = 3/2$, $\mu_I = 2.3817$, $Q = -0.204$							
1.5	5.575[4]	5.564[4]	5.541[4]	5.495[4]	5.450[4]	5.405[4]	5.360[4]
0.5	5.582[4]	5.577[4]	5.566[4]	5.546[4]	5.526[4]	5.506[4]	5.486[4]
–0.5	5.623[4]	5.659[4]	5.732[4]	5.879[4]	6.028[4]	6.179[4]	6.331[4]
–1.5	5.699[4]	5.813[4]	6.044[4]	6.518[4]	7.011[4]	7.522[4]	8.050[4]
$Z = 30$, ^{67}Zn, $I = 5/2$, $\mu_I = 0.875479$, $Q = 0.15$							
2.5	8.251[3]	8.151[3]	7.955[3]	7.569[3]	7.193[3]	6.826[3]	6.470[3]
1.5	8.243[3]	8.137[3]	7.926[3]	7.512[3]	7.110[3]	6.719[3]	6.338[3]
0.5	8.335[3]	8.320[3]	8.290[3]	8.231[3]	8.171[3]	8.112[3]	8.053[3]
–0.5	8.444[3]	8.539[3]	8.729[3]	9.117[3]	9.513[3]	9.917[3]	1.033[4]

TABLE VIII. *(Continued.)*

	$A_{\text{MIT-hfs}}$ (s^{-1})						
M_F	0.05 T	0.1 T	0.2 T	0.4 T	0.6 T	0.8 T	1 T
–1.5	8.570[3]	8.793[3]	9.248[3]	1.019[4]	1.118[4]	1.221[4]	1.329[4]
–2.5	8.800[3]	9.261[3]	1.022[4]	1.228[4]	1.452[4]	1.695[4]	1.958[4]
$Z = 31$, ^{69}Ga, $I = 3/2$, $\mu_I = 2.01659$, $Q = 0.171$							
1.5	6.908[4]	6.894[4]	6.867[4]	6.811[4]	6.756[4]	6.701[4]	6.647[4]
0.5	6.916[4]	6.910[4]	6.897[4]	6.873[4]	6.848[4]	6.824[4]	6.799[4]
–0.5	6.966[4]	7.010[4]	7.098[4]	7.277[4]	7.457[4]	7.640[4]	7.825[4]
–1.5	7.059[4]	7.197[4]	7.476[4]	8.052[4]	8.649[4]	9.268[4]	9.908[4]
$Z = 31$, ^{71}Ga, $I = 3/2$, $\mu_I = 2.56227$, $Q = 0.107$							
1.5	1.116[5]	1.115[5]	1.111[5]	1.104[5]	1.097[5]	1.090[5]	1.083[5]
0.5	1.117[5]	1.116[5]	1.115[5]	1.112[5]	1.109[5]	1.105[5]	1.102[5]
–0.5	1.124[5]	1.129[5]	1.140[5]	1.163[5]	1.186[5]	1.209[5]	1.232[5]
–1.5	1.135[5]	1.153[5]	1.188[5]	1.260[5]	1.335[5]	1.411[5]	1.490[5]
$Z = 32$, ^{73}Ge, $I = 9/2$, $\mu_I = -0.879468$, $Q = -0.196$							
4.5	1.275[4]	1.296[4]	1.338[4]	1.424[4]	1.513[4]	1.604[4]	1.698[4]
3.5	1.278[4]	1.302[4]	1.351[4]	1.451[4]	1.555[4]	1.662[4]	1.773[4]
2.5	1.272[4]	1.289[4]	1.324[4]	1.395[4]	1.468[4]	1.543[4]	1.620[4]
1.5	1.264[4]	1.273[4]	1.292[4]	1.331[4]	1.370[4]	1.410[4]	1.450[4]
0.5	1.256[4]	1.257[4]	1.259[4]	1.264[4]	1.269[4]	1.274[4]	1.278[4]
–0.5	1.247[4]	1.240[4]	1.225[4]	1.196[4]	1.167[4]	1.138[4]	1.110[4]
–1.5	1.238[4]	1.222[4]	1.190[4]	1.126[4]	1.065[4]	1.005[4]	9.469[3]
–2.5	1.229[4]	1.203[4]	1.153[4]	1.055[4]	9.618[3]	8.729[3]	7.882[3]
–3.5	1.218[4]	1.182[4]	1.112[4]	9.783[3]	8.531[3]	7.364[3]	6.283[3]
–4.5	1.198[4]	1.143[4]	1.036[4]	8.392[3]	6.627[3]	5.071[3]	3.722[3]
$Z = 33$, ^{75}As, $I = 3/2$, $\mu_I = 1.43948$, $Q = 0.314$							
1.5	5.925[4]	5.911[4]	5.883[4]	5.828[4]	5.772[4]	5.718[4]	5.663[4]
0.5	5.933[4]	5.927[4]	5.914[4]	5.890[4]	5.865[4]	5.841[4]	5.816[4]
–0.5	5.983[4]	6.028[4]	6.117[4]	6.297[4]	6.480[4]	6.666[4]	6.854[4]
–1.5	6.077[4]	6.216[4]	6.499[4]	7.085[4]	7.696[4]	8.332[4]	8.993[4]
$Z = 34$, ^{77}Se, $I = 1/2$, $\mu_I = 0.535042$, $Q = 0$							
0.5	1.917[4]	1.930[4]	1.958[4]	2.014[4]	2.070[4]	2.128[4]	2.186[4]
–0.5	1.984[4]	2.066[4]	2.236[4]	2.597[4]	2.984[4]	3.399[4]	3.840[4]
$Z = 35$, ^{79}Br, $I = 3/2$, $\mu_I = 2.1064$, $Q = 0.313$							
1.5	2.098[5]	2.095[5]	2.090[5]	2.078[5]	2.067[5]	2.055[5]	2.044[5]
0.5	2.100[5]	2.098[5]	2.096[5]	2.091[5]	2.085[5]	2.080[5]	2.075[5]
–0.5	2.110[5]	2.119[5]	2.137[5]	2.173[5]	2.210[5]	2.247[5]	2.284[5]
–1.5	2.129[5]	2.157[5]	2.214[5]	2.331[5]	2.450[5]	2.572[5]	2.697[5]
$Z = 35$, ^{81}Br, $I = 3/2$, $\mu_I = 2.270562$, $Q = 0.262$							
1.5	2.439[5]	2.436[5]	2.429[5]	2.417[5]	2.405[5]	2.392[5]	2.380[5]
0.5	2.440[5]	2.439[5]	2.436[5]	2.430[5]	2.425[5]	2.419[5]	2.414[5]
–0.5	2.451[5]	2.461[5]	2.481[5]	2.520[5]	2.559[5]	2.599[5]	2.639[5]
–1.5	2.472[5]	2.502[5]	2.564[5]	2.689[5]	2.817[5]	2.948[5]	3.082[5]

D. MIT-hfs results for the whole sequences.

The effect of including both HIT and MIT is illustrated in Figs. 3 and 4 for the Be-like and Ne-like isoelectronic sequences, respectively. It is clear that there is a strong dependence of MIT-hfs rate on the magnetic quantum number M_F of the upper state, when MIT and HIT are of comparable magnitude. For Be-like ions, the hyperfine interaction is the dominant channel for most ions, which results in similar values of MIT-hfs and HIT rates. Only for quite large magnetic-field strengths and for ions in the neutral end of the sequence will the magnetic interaction be important. However, for even atomic numbers the most common isotope has no spin and the MIT will be the dominant effect even for relatively weak magnetic fields.

The trend is significantly different for the Ne-like ions, as shown in Fig. 4, especially at large field strength. The M_F dependence feature will result in a significant difference in lifetimes associated with different transition channels. The B field and Z dependence of MIT-hfs rates provide the possibility of different candidate ions for different experimental facilities based on their field strength, e.g., ion storage ring, EBIT, and Tokamak, for future experimental studies. It is interesting to note that in spite of the fact that the MIT-fs has been observed in Ne-like argon and iron, no results have been published on odd isotopes, where the HIT dominates for even high-Z ions. Especially in light of the uncertain situation for Be-like HITs, we call for attempts to measure the HIT in Ne-like ions.

It can be easily seen from Figs. 2–4 that the magnetic interaction has a stronger effect on Ne-like ions than for Be-like ions. As described in Eqs. (16)–(20), the MITs rates depend on the mixing coefficients and the allowed transition rates. The mixing coefficients are proportional to the square of the reduced magnetic interaction matrix elements. For the two atomic systems discussed in this work, the MIT transition $^3P_0$-$^1S_0$ is introduced by the mixing between $^3P_0$ and two perturbers $^1P_1$ and $^3P_1$. For the Ne-like ions, which have the reversed ^3P levels, changing from LS- toward jj-coupling conditions along the isoelectronic sequence, the interaction with the $^1P_1$ is one order of magnitude larger than that of Be-like ions. On the other hand, the intercombination transitions $^3P_1$-$^1S_0$ of Ne-like ions have a rate of four orders of magnitude larger than Be-like ions. Due to the two reasons above, for the same magnetic-field strength, the magnetic interaction is larger for the Ne-like ions than for the Be-like ions.

Finally, we give in Tables VII (Be-like ions) and VIII (Ne-like ions) the resulting $A_{\text{MIT-hfs}}$ for isotopes with nuclear spin and in magnetic-field strengths of 0.05, 0.1, 0.2, 0.4, 0.6, 0.8, and 1 T. We only include some ions for the Be-like sequence, but the full sequence, as well as results for both sequences for other magnetic fields, are available from the authors.

V. CONCLUSION

We have performed large-scale calculations of the transition properties and presented a systematic study of MIT-hfs using the MCDHF method for Be-like ($5 \leqslant Z \leqslant 73$) and Ne-like ($11 \leqslant Z \leqslant 35$) ions. There is good agreement between the resulting MIT-fs and HIT rates with earlier theoretical ones for most of the Be- and Ne-like ions.

We compared the theoretical MIT-hfs values with available experimental results and concluded that the effect from magnetic field on the HIT rates in Be-like ions is significant at certain magnetic-field strength, especially for ions at the low-Z end of the isoelectronic sequence. However, the reasons for the discrepancies for Be-like ^{33}S and ^{47}Ti are still unclear. Future experimental studies are called for to extract the reasons for the disagreements and benchmark the theoretical work. At the same time, the Ne-like results for Ar and Fe are in agreement between theory and experiment, so we here call for experimental investigations for species with odd atomic number, to test the calculations for HIT.

ACKNOWLEDGMENTS

This work was supported by the Swedish Research Council (VR) under Contract No. 2015-04842 and National Natural Science Foundation of China Contract No. 11474069.

[1] T. Brage, M. Andersson, and R. Hutton, AIP Conf. Proc. **1125**, 18 (2009).
[2] J. Grumer, T. Brage, M. Andersson, J. Li, P. Jönsson, W. Li, Y. Yang, R. Hutton, and Y. Zou, Phys. Scr. **89**, 114002 (2014).
[3] T. Brage, P. G. Judge, A. Aboussaïd, M. R. Godefroid, P. Jönsson, A. Ynnerman, C. F. Fischer, and D. S. Leckrone, Astrophys. J. **500**, 507 (1998).
[4] F. P. Keenan, P. L. Dufton, W. A. Feibelman, K. L. Bell, A. Hibbert, and R. P. Stafford, Astrophys. J. **423**, 882 (1994).
[5] D. Porquet, R. Mewe, J. Dubau, A. J. J. Raasen, and J. S.Kaastra, Astron. Astrophys **376**, 1113 (2001).
[6] J. Li, J. Grumer, W. Li, M. Andersson, T. Brage, R. Hutton, P. Jönsson, Y. Yang, and Y. Zou, Phys. Rev. A **88**, 013416 (2013).
[7] J. Grumer, W. Li, D. Bernhardt, J. Li, S. Schippers, T. Brage, P. Jönsson, R. Hutton, and Y. Zou, Phys. Rev. A **88**, 022513 (2013).
[8] W. Li, J. Grumer, Y. Yang, T. Brage, K. Yao, C. Chen, T. Watanabe, P. Jönsson, H. Lundstedt, R. Hutton *et al.*, Astrophys. J. **807**, 69 (2015).
[9] P. Beiersdorfer, J. H. Scofield, and A. L. Osterheld, Phys. Rev. Lett. **90**, 235003 (2003).
[10] P. Beiersdorfer, J. R. C. López-Urrutia, and E. Träbert, Astrophys. J. **817**, 67 (2016).
[11] W. Li, Y. Yang, B. Tu, J. Xiao, J. Grumer, T. Brage, T. Watanabe, R. Hutton, and Y. Zou, Astrophys. J. **826**, 219 (2016).
[12] J. P. Marques, F. Parente, and P. Indelicato, Phys. Rev. A **47**, 929 (1993).
[13] W. R. Johnson, K. T. Cheng, and D. R. Plante, Phys. Rev. A **55**, 2728 (1997).
[14] M. Andersson, Y. Liu, C. Y. Chen, R. Hutton, Y. Zou, and T. Brage, Phys. Rev. A **78**, 062505 (2008).
[15] M. Andersson, K. Yao, R. Hutton, Y. Zou, C. Y. Chen, and T. Brage, Phys. Rev. A **77**, 042509 (2008).
[16] M. Andersson, Y. Zou, R. Hutton, and T. Brage, Phys. Rev. A **79**, 032501 (2009).
[17] H. Kang, J. Li, C. Dong, P. Jönsson, and G. Gaigalas, J. Phys. B: At., Mol. Opt. Phys. **42**, 195002 (2009).
[18] W. Johnson and U. Safronova, *40th Annual Meeting of the APS Division of Atomic, Molecular and Optical Physics*, in Bulletin of the American Physical Society, Charlottesville, Virginia, May 19–23, 2009, Volume 54 (The American Physical Society, 2009).
[19] M. Andersson, Y. Zou, R. Hutton, and T. Brage, J. Phys. B: At., Mol. Opt. Phys. **43**, 095001 (2010).
[20] M. Andersson, J. Grumer, T. Brage, Y. Zou, and R. Hutton, Phys. Rev. A **93**, 032506 (2016).
[21] L. Engström, C. Jupen, B. Denne, S. Huldt, W. T. Meng, P. Kaijser, U. Litzen, and I. Martinson, J. Phys. B: At., Mol. Opt. Phys. **13**, L143 (1980).
[22] B. Denne, S. Huldt, J. Pihl, and R. Hallin, Phys. Scr. **22**, 45 (1980).
[23] A. Livingston and S. Hinterlong, Nucl. Instrum. Methods, Phys. Res. **202**, 103 (1982).
[24] R. Marrus, A. Simionovici, P. Indelicato, D. D. Dietrich, P. Charles, J.-P. Briand, K. Finlayson, F. Bosch, D. Liesen, and F. Parente, Phys. Rev. Lett. **63**, 502 (1989).
[25] R. W. Dunford, H. G. Berry, D. A. Church, M. Hass, C. J. Liu, M. L. A. Raphaelian, B. J. Zabransky, L. J. Curtis, and A. E. Livingston, Phys. Rev. A **48**, 2729 (1993).
[26] P. Indelicato, B. B. Birkett, J.-P. Briand, P. Charles, D. D. Dietrich, R. Marrus, and A. Simionovici, Phys. Rev. Lett. **68**, 1307 (1992).

[27] B. B. Birkett, J.-P. Briand, P. Charles, D. D. Dietrich, K. Finlayson, P. Indelicato, D. Liesen, R. Marrus, and A. Simionovici, Phys. Rev. A **47**, R2454 (1993).
[28] S. Toleikis, B. Manil, E. Berdermann, H. F. Beyer, F. Bosch, M. Czanta, R. W. Dunford, A. Gumberidze, P. Indelicato, C. Kozhuharov *et al.*, Phys. Rev. A **69**, 022507 (2004).
[29] J. G. Li, P. Jönsson, G. Gaigalas, and C. Z. Dong, Eur. Phys. J. D **51**, 313 (2009).
[30] E. Träbert, P. Beiersdorfer, G. V. Brown, K. Boyce, R. L. Kelley, C. A. Kilbourne, F. S. Porter, and A. Szymkowiak, Phys. Rev. A **73**, 022508 (2006).
[31] K. Yao, M. Andersson, T. Brage, R. Hutton, P. Jönsson, and Y. Zou, Phys. Rev. Lett. **97**, 183001 (2006).
[32] E. Träbert, P. Beiersdorfer, and G. V. Brown, Phys. Rev. Lett. **98**, 263001 (2007).
[33] T. Brage, P. G. Judge, and C. R. Proffitt, Phys. Rev. Lett. **89**, 281101 (2002).
[34] S. Schippers, D. Bernhardt, A. Müller, M. Lestinsky, M. Hahn, O. Novotný, D. W. Savin, M. Grieser, C. Krantz, R. Repnow *et al.*, Phys. Rev. A **85**, 012513 (2012).
[35] S. Schippers, E. W. Schmidt, D. Bernhardt, D. Yu, A. Müller, M. Lestinsky, D. A. Orlov, M. Grieser, R. Repnow, and A. Wolf, Phys. Rev. Lett. **98**, 033001 (2007).
[36] T. Rosenband, P. O. Schmidt, D. B. Hume, W. M. Itano, T. M. Fortier, J. E. Stalnaker, K. Kim, S. A. Diddams, J. C. J. Koelemeij, J. C. Bergquist *et al.*, Phys. Rev. Lett. **98**, 220801 (2007).
[37] J. Li, C. Dong, P. Jönsson, and G. Gaigalas, Phys. Lett. A **375**, 914 (2011).
[38] P. Jönsson, F. Parpia, and C. Fischer, Comput. Phys. Commun. **96**, 301 (1996).
[39] K. T. Cheng, M. H. Chen, and W. R. Johnson, Phys. Rev. A **77**, 052504 (2008).
[40] K. T. Cheng and W. J. Childs, Phys. Rev. A **31**, 2775 (1985).
[41] M. Andersson and P. Jönsson, Comput. Phys. Commun. **178**, 156 (2008).
[42] W. Johnson, Can. J. Phys. **89**, 429 (2011).
[43] P. Jönsson, G. Gaigalas, J. Bieroń, C. F. Fischer, and I. Grant, Comput. Phys. Commun. **184**, 2197 (2013).
[44] I. P. Grant, *Relativistic Quantum Theory of Atoms and Molecules* (Springer, New York, 2007).
[45] C. F. Fischer, M. Godefroid, T. Brage, P. Jönsson, and G. Gaigalas, J. Phys. B: At., Mol. Opt. Phys. **49**, 182004 (2016).
[46] I. Grant, B. McKenzie, P. Norrington, D. Mayers, and N. Pyper, Comput. Phys. Commun. **21**, 207 (1980).
[47] I. P. Grant, J. Phys. B: At., Mol. Opt. Phys. **7**, 1458 (1974).
[48] M. H. Chen, K. T. Cheng, and W. R. Johnson, Phys. Rev. A **64**, 042507 (2001).
[49] B. O. Roos, P. R. Taylor, and P. E. Sigbahn, Chem. Phys. **48**, 157 (1980).
[50] J. Olsen, B. O. Roos, P. Jorgensen, and H. J. A. Jensen, J. Chem. Phys. **89**, 2185 (1988).
[51] T. Brage and C. F. Fischer, Phys. Scr. **1993**, 18 (1993).
[52] S. Verdebout, C. Nazé, P. Jönsson, P. Rynkun, M. Godefroid, and G. Gaigalas, At. Data Nucl. Data Tables **100**, 1111 (2014).
[53] P. Jönsson, P. Bengtsson, J. Ekman, S. Gustafsson, L. Karlsson, G. Gaigalas, C. F. Fischer, D. Kato, I. Murakami, H. Sakaue *et al.*, At. Data Nucl. Data Tables **100**, 1 (2014).
[54] C. Froese-Fischer, T. Brage, and P. Jönsson, *Computational Atomic Structure: An MCHF Approach* (Taylor & Francis, London, 1997).
[55] Y. Ralchenko, A. E. Kramida, J. Reader, and NIST ASD Team (2008). NIST Atomic Spectra Database (version 3.1.5), available at http://physics.nist.govasd3 [Nov. 27 2008]. National Institute of Standards and Technology, Gaithersburg, MD.
[56] N. J. Stone, IAEA Vienna Report No. INDC(NDS)-0658, 2014.
[57] J. Li and C. Dong, Plasma Sci. Technol. **12**, 364 (2010).